OAK RIDGE NATIONAL LABORATORY
OPERATED BY
UNION CARBIDE CORPORATION
NUCLEAR DIVISION
POST OFFICE BOX X
OAK RIDGE, TENNESSEE 37830

ORNL/MIT-254

DATE: May 19, 1977

SUBJECT: Parameters Influencing Dispersion in a Three-Phase Fluidized Bed

TO: Distribution List

FROM: R.S. Cherry, A.C. Sharon, and Z.P. Chen*

Consultants: J.M. Begovich, S.D. Clinton, and J.S. Watson

ABSTRACT

The effects of liquid and gas superficial velocity, solids loading, and particle diameter on axial dispersion in a three-phase fluidized bed were investigated. Gas velocities of 4-16 cm/sec and liquid velocities of 4-12 cm/sec through the 7.62-cm-ID bed were utilized with 1.5, 2.25, and 3.0 kg loadings of 0.32 and 0.46-cm-diam glass beads. Larger beads (0.62-cm-diam) were fluidized with the same range of gas velocities but at liquid velocities of 5-12 cm/sec and at a 1.5-kg loading. Dispersion coefficients were calculated by analyzing the spread of an injected tracer with three methods: an analysis of moments, a modified analysis of moments, and a transfer function. There is excellent agreement among the three methods when applied to symmetrical, idealized data. However, the agreement is very poor when the methods are applied to experimental data. Several modifications in the column design and tracer monitoring apparatus are suggested.

---

*Rewritten by W.M. Ayers

Oak Ridge Station
School of Chemical Engineering Practice
Massachusetts Institute of Technology
W.M. Ayers, Director

Printed in the United States of America. Available from
National Technical Information Service
U.S. Department of Commerce
5285 Port Royal Road, Springfield, Virginia 22161
Price: Printed Copy $4.~~00~~ 50; Microfiche $3.00

Contents

1. SUMMARY

The effects of liquid and gas superficial velocity, solids loading, and particle diameter on axial dispersion in a three-phase fluidized bed were investigated in a 7.62-cm-ID x 152 cm plexiglas column. Glass beads of 0.32, 0.46, and 0.62-cm-diam were fluidized with water and air at 3-12 and 4-16 cm/sec, respectively. One and one-half, 2.25, and 3.0-kg bead loadings were utilized.

Variations in the liquid conductivity from pulsed injections of potassium chloride were measured at two positions within the column to determine the degree of axial dispersion. The spread of the electrolyte tracer as it passed the two measuring points was quantified with an analysis of moments, modified analysis of moments and transfer function techniques. The agreement among the three methods in analyzing experimental data was poor and no clear correlation between the dispersion coefficient, fluid velocities, particle size, and mass loading was apparent. It is recommended that the gas and liquid distributor be redesigned and the tracer detection electrodes be moved further from the entrance so that reproducible data may be obtained.

2. INTRODUCTION

Fluidized bed reactors, operating between the extremes of well-mixed and plug flow behavior, are often characterized as operating in axially dispersed plug flow. The dispersion coefficient used to quantify the amount of mixing in this type of flow includes the effects of both diffusion and turbulent mixing. This coefficient may be determined through analysis of the broadening of an injected pulse of tracer fluid as it passes through the reactor (3,4). Calculation of the dispersion coefficient by an analysis of the first and second moments of the tracer concentration history resulting from a perfect input pulse was developed by Levenspiel and Smith (9). Van der Láan (15) expanded their work to cover a variety of boundary conditions and Aris (1), corrected by Bischoff (3), showed that an imperfect tracer pulse could be accounted for by measuring the tracer concentration at two different positions in the system. Ostergaard and Michelsen developed methods to calculate the dispersion coefficient based on a transfer function (the ratio of Laplace transforms of tracer concentration histories at two positions along the column) and a modification of the analysis of moments technique (10,11).

Several MIT Practice School groups have studied various aspects of three-phase fluidized beds. Saad *et al.* (14) derived plug flow, well-mixed, and dispersed flow models for determining the bed mass transfer coefficient and calculated mass transfer coefficients assuming the plug flow model. Burck *et al.* (5) correlated solid holdup to minimum fluidization velocity and also calculated mass transfer coefficients by assuming a dispersion coefficient in a trial and error solution. Khosrowshahi *et al.* (7) correlated the solid phase holdup with the Reynolds and Archimedes number and studied the hydrodynamic variables affecting minimum fluidization. Most recently, Christman *et al.* (6) attempted to determine dispersion coefficients for the apparatus used in this study with both the analysis of moments and transfer function methods.

The objective of this study was to determine the effect of gas and liquid superficial velocities, mass loadings, and particle diameters on dispersion in a fluidized bed and to compare the dispersion coefficients calculated with the traditional analysis of moments technique, the transfer function technique, and Ostergaard and Michelsen's modified analysis of moments technique.

3. THEORY

Dispersion in flow systems may be measured by tracer tests in which a pulse, step, sinusoidal or random concentration input is introduced into the system and the concentration monitored downstream as a function of time. The equation describing the tracer concentration variation with time and distance along the column is

$$D\frac{\partial^2 C}{\partial z^2} - U_L\frac{\partial C}{\partial z} = \frac{\partial C}{\partial t} \qquad (1)$$

With L_e defined as the distance between tracer input and measuring point for perfect pulse inputs or the distance between measuring points for imperfect tracer injections, a Peclet number, Pe, may be defined as $U_L L_e/D$, a dimensionless distance as (z/L_e), and the time variable as (L_e/U_L) so that equation (1) can be written as:

$$\frac{1}{Pe}\frac{\partial^2 C}{\partial z_*^2} - \frac{\partial C}{\partial z_*} = \tau\frac{\partial C}{\partial t} \qquad (2)$$

For a pulse input to a doubly infinite open system, i.e., a flow system of infinite length with no change in the flow characteristics at the boundaries of the section under consideration, the dimensionless variance, σ_θ^2, of the output tracer concentration time curve is related to the Péclet number by the relation (9),

$$\sigma_\theta^2 = \frac{\sigma^2}{\tau^2} = \frac{2}{Pe} + \frac{8}{Pe^2} \tag{3}$$

In actual systems, it is impossible to introduce a perfect pulse input. In such a situation the Peclet number may be calculated by using the difference in variance of tracer concentration curves at two positions with the expression (1,3)

$$\Delta\sigma_\theta^2 = \frac{\sigma_2^2 - \sigma_1^2}{\tau^2} = \frac{2}{Pe} \tag{4}$$

Calculation of the residence time between electrodes for the imperfect tracer method may be performed by taking the difference between the means of the input and output curves. Calculation of the mean, $\bar{t}$, of a concentration time curve is done by numerical evaluation of the equation

$$\bar{t} = \int_0^\infty tC(t)\,dt \Big/ \int_0^\infty C(t)\,dt \tag{5}$$

$$\simeq \sum_0^\infty tC(t)\Delta t \Big/ \sum_0^\infty C(t)\Delta t \tag{6}$$

The variance of the curve is calculated in the same manner:

$$\sigma^2 = \int_0^\infty (t - \bar{t})^2 C(t)\,dt \Big/ \int_0^\infty C(t)\,dt \tag{7}$$

$$= \sum_0^\infty (t - \bar{t})^2 C(t)\Delta t \Big/ \sum_0^\infty C(t)\Delta t \tag{8}$$

The two tracer concentration-time curves measured at different positions commonly display tailing as well as random fluctuations. Although the random fluctuations exist at all points on the concentration curve, they contribute to a large percentage error in determining the actual tracer concentration near the tail of the curve. These concentration values are multiplied by a large value of $(t - \bar{t})^2$ in evaluating σ^2. Thus, depending on the overall accuracy of these measurements, the variance and hence the Peclet number may be incorrectly determined.

Ostergaard and Michelsen have proposed a method to reduce the effect of these inaccuracies by taking the Laplace transform of the tracer concentration curves measured at two positions in the test section (11).

$$\mathcal{L}[C(t)] = C(s) = \int_0^\infty C(t)\exp(-st)dt \qquad (9)$$

This reduces the effect of errors at low concentrations obtained at large times. The system can then be characterized by a transfer function, F(s), which is the ratio of normalized Laplace transforms of the response to the tracer input at the two measuring positions.

$$F(s) = \frac{C_2(s)}{C_1(s)} = \frac{\int_0^\infty C_2(t)\exp(-st)dt \Big/ \int_0^\infty C_2(t)dt}{\int_0^\infty C_1(t)\exp(-st)dt \Big/ \int_0^\infty C_1(t)dt} \qquad (10)$$

The functional form of the transfer function may be determined analytically from Eq.(2). Evaluating the transfer function at two tracer measuring points ($z_*= 0$ and $z_*= 1$) one obtains:

$$F(s) = \frac{C(s)_{z_*=1}}{C(s)_{z_*=0}} = \exp[\frac{Pe}{2}(1-(1+\frac{4s\tau}{Pe})^{1/2}] \qquad (11)$$

If F(s) is calculated by integration of the tracer curves for two values of s, Eq. (11) may be solved for the two variables Pe and τ. They may also be obtained by finding F(s) for more than two values of s and statistically analyzing the results for Pe and τ. This may be accomplished by rearranging Eq. (11) to give

$$[\ln (\frac{1}{F(s)})]^{-1} = \tau s[\ln (\frac{1}{F(s)})]^{-2} - \frac{1}{Pe} \qquad (12)$$

By plotting $[\ln \frac{1}{F(s)}]^{-1}$ against $s[\ln \frac{1}{F(s)}]^{-2}$, a straight line with slope τ and intercept -1/Pe should result.

In a variation of this technique, the Laplace transform of a concentration distribution, Eq. (9), may be differentiated with respect to s to give,

$$\frac{d^nC(s)}{ds^n} = (-1)^n\int_0^\infty t^nC(t)\exp(-st)dt \Big/ \int_0^\infty C(t)dt \qquad (13)$$

Defining the transform mean and transform moments as:

$$\bar{t}_s = \int_0^\infty tC(t)\exp(-st)dt \Big/ \int_0^\infty C(t)\exp(-st)dt \tag{14}$$

$$c_S^{[n]} = \int_0^\infty (t - \bar{t}_s)^n C(t)\exp(-st)dt \Big/ \int_0^\infty C(t)\exp(-st)dt \tag{15}$$

it may be shown (11) that:

$$\frac{-F's}{F(s)} = \bar{t}_{(2)_s} - \bar{t}_{(1)_s} \tag{16}$$

$$\frac{d}{ds}\left(\frac{F'(s)}{F(s)}\right) = c_{(2)_s}^2 - c_{(1)_s}^2 \tag{17}$$

$$-\frac{d^2}{ds^2}\left(\frac{F'(s)}{F(s)}\right) \doteq c_{(2)_s}^3 - c_{(1)_s}^3 \tag{18}$$

From Eq. (11),

$$\frac{F'(s)}{F(s)} = -\tau\left(1 + \frac{4st}{Pe}\right)^{-1/2} \tag{19}$$

$$\frac{d^n}{ds^n}\left(\frac{F'(s)}{F(s)}\right) = (-\tau)^{n+1} Pe^{-n} \frac{(2n)!}{n!} \left(1 + \frac{4s\tau}{Pe}\right)^{-n-1/2} \tag{20}$$

The Peclet number and τ may now be calculated using two values of s and Eqs. (14) or (15) in Eqs. (16), (17), or (18) (or higher derivatives) to evaluate F'(s)/F(s). Alternatively, for one value of s, two moments may be calculated by numerical integration of Eqs. (14) and (15) and then solving for τ and Pe with Eqs. (16) through (20).

4. APPARATUS AND PROCEDURE

4.1 Apparatus

The three-phase fluidized bed consists of a 5-ft-high, 3-in.-ID, Plexiglas tube loaded with glass beads suspended by a cocurrent upward flow of air and water (Fig. 1). A centrifugal pump introduces water through a rotameter into the bottom of the column from a 55-gal storage tank. A Plexiglas disc with 1/8-in.-diam holes serves as a liquid distributor and as a support for the static solids bed. Air is fed through a rotameter and into the column from laboratory air lines and distributed via the same Plexiglas disc. Water exits the column through a T-tube equipped with a stainless steel screen to catch any beads which may be carried to the top of the column. The T-tube arrangement also

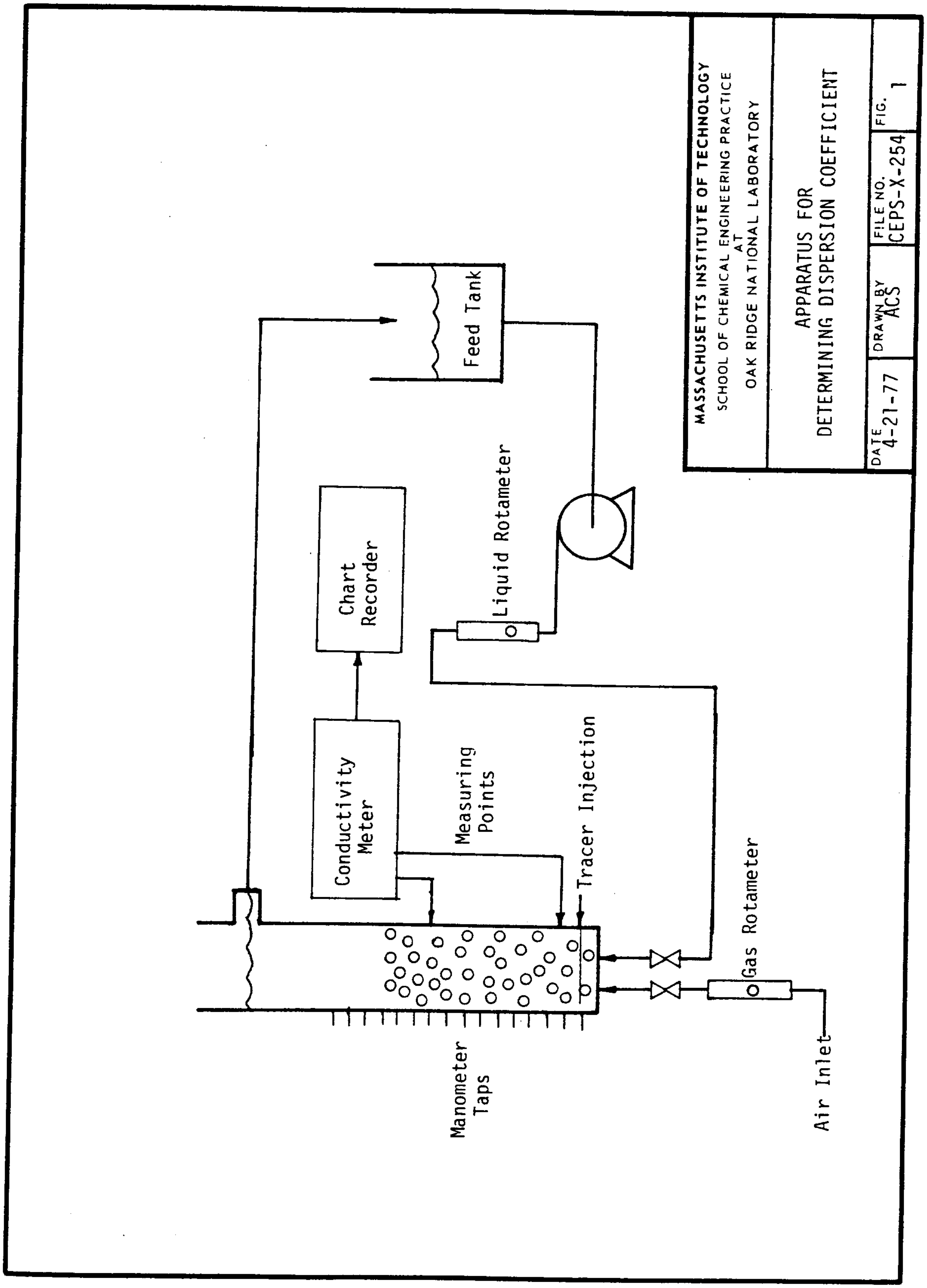
Feed Tank
Chart Recorder
Liquid Rotameter
Conductivity Meter
Measuring Points
Tracer Injection
Gas Rotameter
Manometer Taps
Air Inlet
MASSACHUSETTS INSTITUTE OF TECHNOLOGY
SCHOOL OF CHEMICAL ENGINEERING PRACTICE
AT
OAK RIDGE NATIONAL LABORATORY
APPARATUS FOR
DETERMINING DISPERSION COEFFICIENT
DATE 4-21-77
DRAWN BY ACS
FILE NO. CEPS-X-254
FIG. 1

maintains a constant liquid level in the column. Sixteen water manometers are connected to ports at 8-cm intervals up the column beginning one centimeter above the distributor plate. A mercury manometer is connected to the air feed line to monitor the pressure drop through the column.

One-sixth second pulses of saturated aqueous potassium chloride tracer were injected into the column 7 cm above the distributor plate through a 1/8-in.-diam, 2.5-in.-long stainless steel tube that has six holes drilled into it in the plane of a column cross section. A solenoid valve can be set to control the duration of the pulse, and a regulator to control the air pressure used to inject the tracer. The tracer concentration is monitored at 8 cm above the injection point and at a variable distance above that by two sets of platinum electrodes connected to conductivity meters. Conductivity meter output is recorded on a dual pen chart recorder.

4.2 Experimental Procedure

The operating conditions for each experiment are listed in Table 1. After loading the glass beads into the column, the static bed height was measured, and the bed was fluidized with water and air. For each operating condition, water temperature, rotameter settings, and the readings of the sixteen water manometers were recorded. The total pressure drop across the column as displayed by a mercury manometer was reported for each run in which gas was introduced to the bed. For cases of no gas flow, the manometer was isolated from the column by a shut-off valve. The bed height was calculated by plotting the pressures from the sixteen manometers and determining the point of intersection between the two best straight line s through points in and above the bed. Tracer concentration histories, monitored at the two electrodes, were digitized and punched onto paper tape using an Elographics digitizer connected to a teletype. Approximately forty points per curve were taken. Data for each run were input onto disc files on the ORNL PDP-10 to form the data base for a program which calculated Peclet numbers, dispersion coefficients, residence times, holdups, fluid velocities and the Reynolds number.

5. RESULTS AND DISCUSSION

5.1 Liquid Volume Fractions

Experimentally determined liquid holdups with only water in the column (no beads and no air flow rate) are presented in Fig. 2. With only liquid present the holdup should be unity at all flow rates. For liquid velocities above about 3 cm/sec, the values determined by tracer tests using the analysis of moments are within 10% of this value; whereas, below 3 cm/sec the holdups are quite significantly lower. This might be explained by assuming a laminar to turbulent flow transition occurs at about 3 cm/sec. Calculation of the Reynolds number with a density of 1 gm/cm^3,

TABLE 1: OPERATING CONDITIONS FOR DETERMINATION OF DISPERSION COEFFICIENTS

	Glass Bead Diameter (cm)		
Loading (kg)	0.32	0.46	0.62
1.50	✓	✓	✓
2.25	✓	✓	
3.00	✓	✓	
Liquid Superficial Velocity (cm/sec)			
3.2	✓		
4.1	✓	✓	
4.9			✓
6.0	✓	✓	✓
8.0	✓	✓	✓
10.0		✓	✓
12.0	✓	✓	✓

Gas superficial velocities were 0, 4, 12, and 16 cm/sec for each liquid superficial velocity.

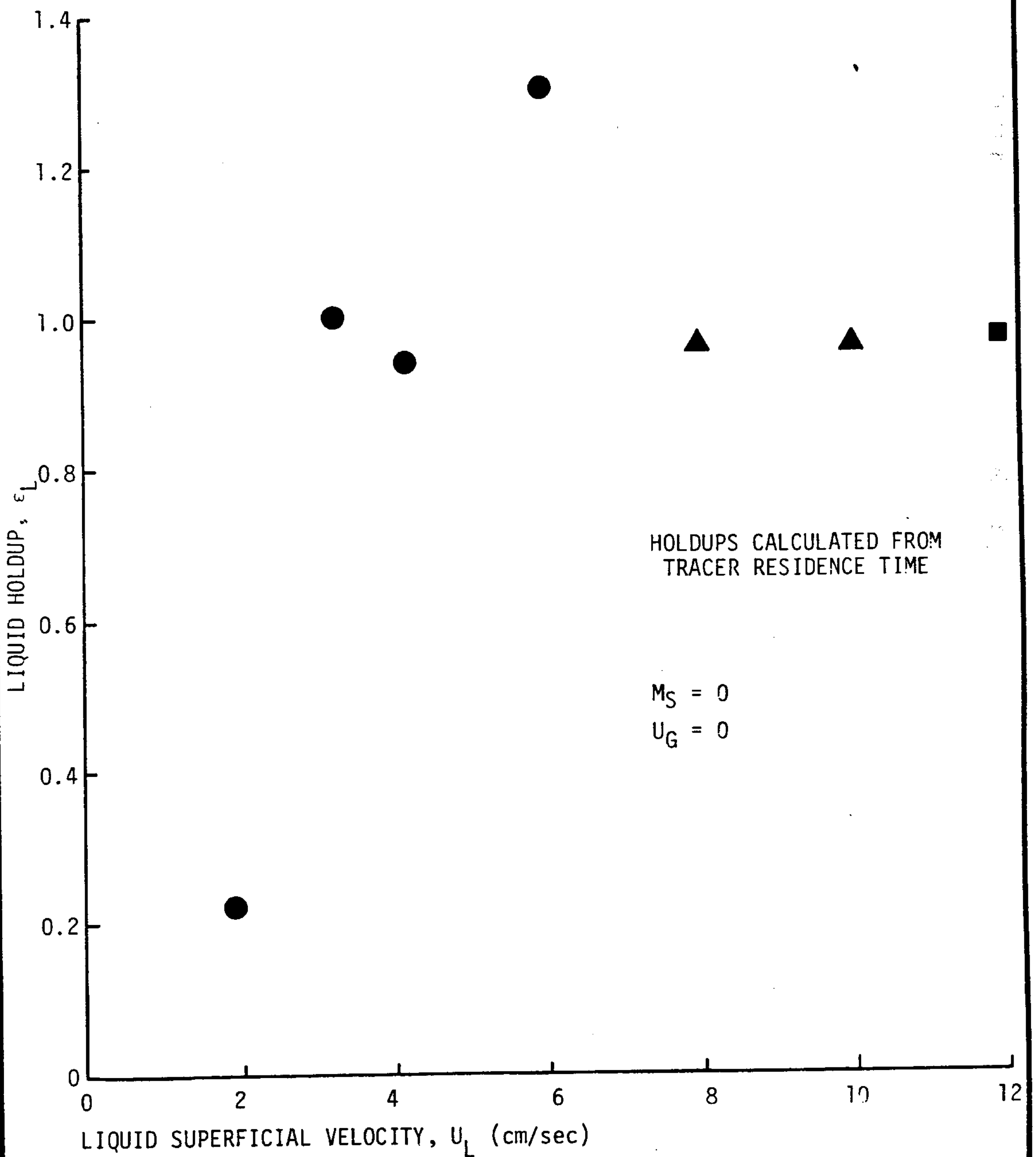

MASSACHUSETTS INSTITUTE OF TECHNOLOGY
SCHOOL OF CHEMICAL ENGINEERING PRACTICE
AT
OAK RIDGE NATIONAL LABORATORY

VARIATION OF LIQUID HOLDUP WITH LIQUID SUPERFICIAL VELOCITY

DATE	DRAWN BY	FILE NO.	FIG.
4/21/77	REB	CEP-X-254	2

velocity of 3 cm/sec, diameter of 7.62 and viscosity of 0.01 poise gives a value of ∿2286 which is greater than the value for laminar-turbulent transitions in tubes, assuming no entrance effects (entrance length = 0.035dRe = 609 cm) (2). Lower holdups would be obtained if laminar flow exists since the tracer, distorted by the velocity profile, would reach the second electrode faster than expected from the superficial velocity.

Plots of liquid and liquid plus gas holdups are presented in Figs. 3, 4 and 5 for 1.5 and 3.0 kg loading of 0.46 cm glass beads. While liquid holdup in most cases decreases with superficial gas velocity, the liquid plus gas holdup increases. Ostergaard and Theisen (13) suggest that much of the liquid passes through the bed in the wake of gas bubbles, thus decreasing interstitial liquid velocity in the remainder of the bed. Such a decrease would result in bed contraction. Fig. 4, however, demonstrates that the bed continues to expand after the introduction of gas to the bed. In Fig. 5, data at the same operating conditions as in Fig. 3 is presented for comparison of the two methods for calculating the holdups. The discrepancy between the two methods increases with the liquid flowrate. Figures6 and 7 show the effects of solids loading and particle diameter on the liquid holdup: Fig. 6 with no gas flowrate and Fig. 7 with a gas superficial velocity of 15.8 cm/sec. The increase in the liquid holdup with liquid velocity and the absence of a discernable influence of the solids loading was expected. Increasing the particle diameter increases the minimum fluidization velocity. Therefore, at a given flowrate, the excess flowrate over the minimum fluidization velocity should be less for the larger diameter beads which should result in smaller liquid holdups. This is not apparent in Figs. 6 or 7. The error associated with the holdup measurements is discussed in Section 5.3.

5.2 Dispersion Coefficients

Dispersion coefficients calculated by each of the three methods are presented in Table 2 for a bed loading of 3 kg of 0.46-cm glass beads. In general, the three methods result in three different dispersion values for the same data. A similar listing of the results (Table 3) for 3 kg of 0.32-cm glass beads shows the same scattered behavior for the three methods. This behavior is typical of all the data analyzed (Appendix 10.2).

Due to the disagreement among the three methods of determining the dispersion coefficient, only the method of moments was used to consider the variation of dispersion with various experimental parameters. Fig. 8 is a plot of dispersion versus superficial liquid and gas velocity. As noted by Christman *et. al.* (6), dispersion often increases with superficial liquid velocity until a sharp decrease occurs. Also shown in Fig. 8 is an apparent increase in dispersion when gas is introduced to the column although there is no clear relation between the dispersion coefficient and the superficial gas velocity.

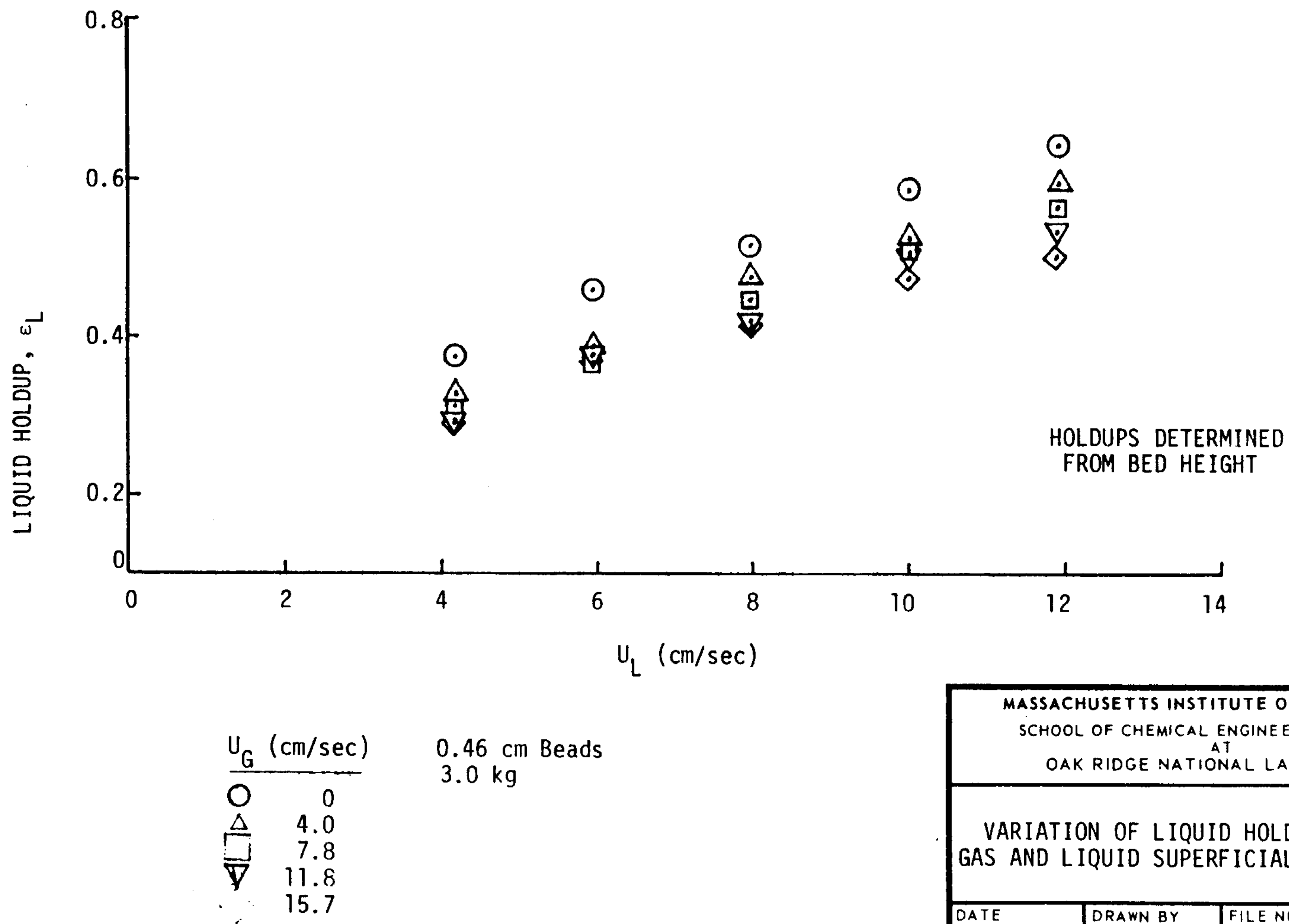

MASSACHUSETTS INSTITUTE OF TECHNOLOGY
SCHOOL OF CHEMICAL ENGINEERING PRACTICE
AT
OAK RIDGE NATIONAL LABORATORY

VARIATION OF LIQUID HOLDUP WITH GAS AND LIQUID SUPERFICIAL VELOCITY

DATE	DRAWN BY	FILE NO.	FIG.
4/21/77	REB	CEP-X-254	3

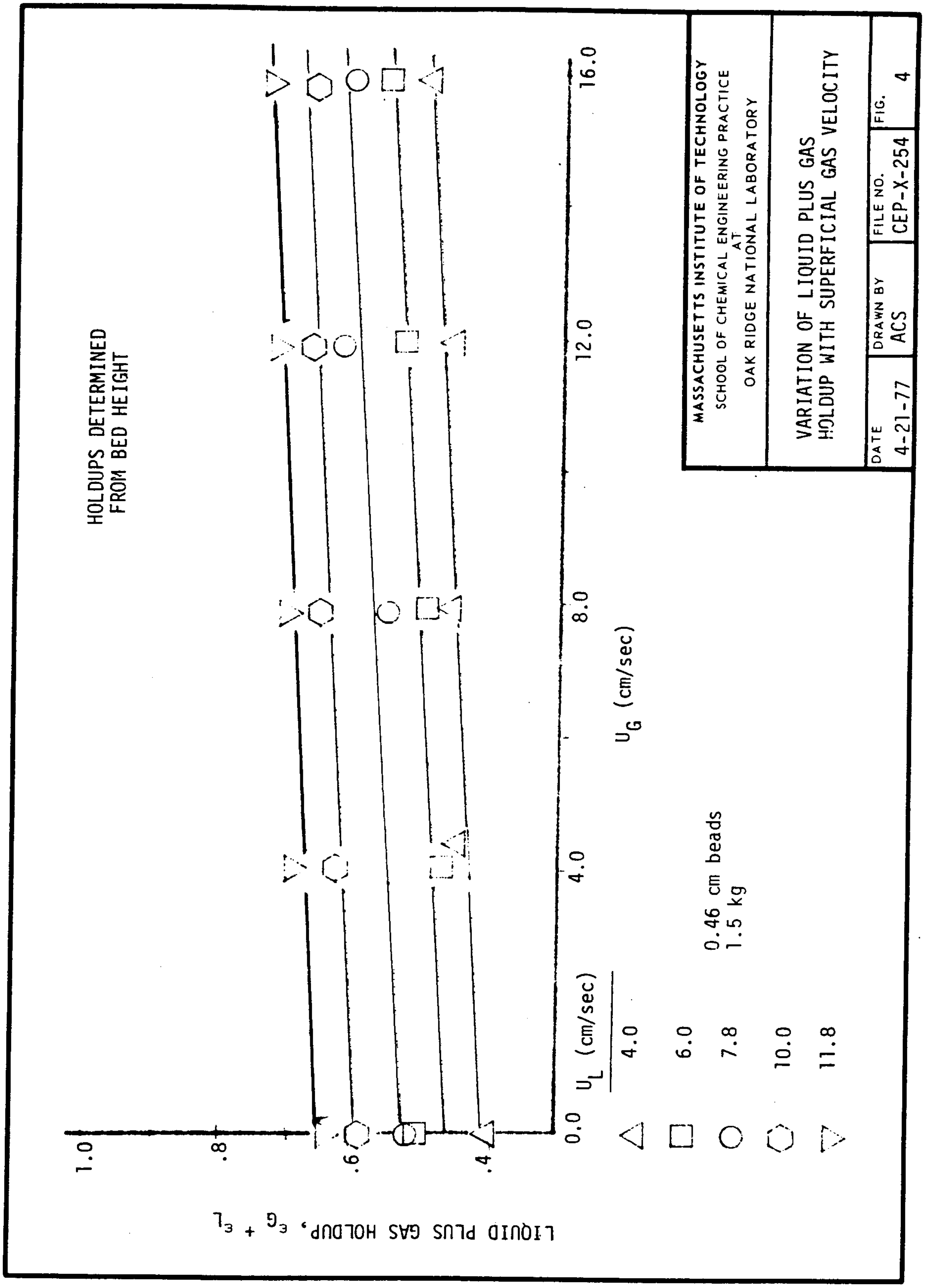
HOLDUPS DETERMINED
FROM BED HEIGHT
1.0
.8
.6
.4
0.0
4.0
8.0
12.0
16.0
U_G (cm/sec)
LIQUID PLUS GAS HOLDUP, $\epsilon_G + \epsilon_L$
U_L (cm/sec)
4.0
6.0
7.8
10.0
11.8
0.46 cm beads
1.5 kg
MASSACHUSETTS INSTITUTE OF TECHNOLOGY
SCHOOL OF CHEMICAL ENGINEERING PRACTICE
AT
OAK RIDGE NATIONAL LABORATORY
VARIATION OF LIQUID PLUS GAS
HOLDUP WITH SUPERFICIAL GAS VELOCITY
DATE
4-21-77
DRAWN BY
ACS
FILE NO.
CEP-X-254
FIG.
4

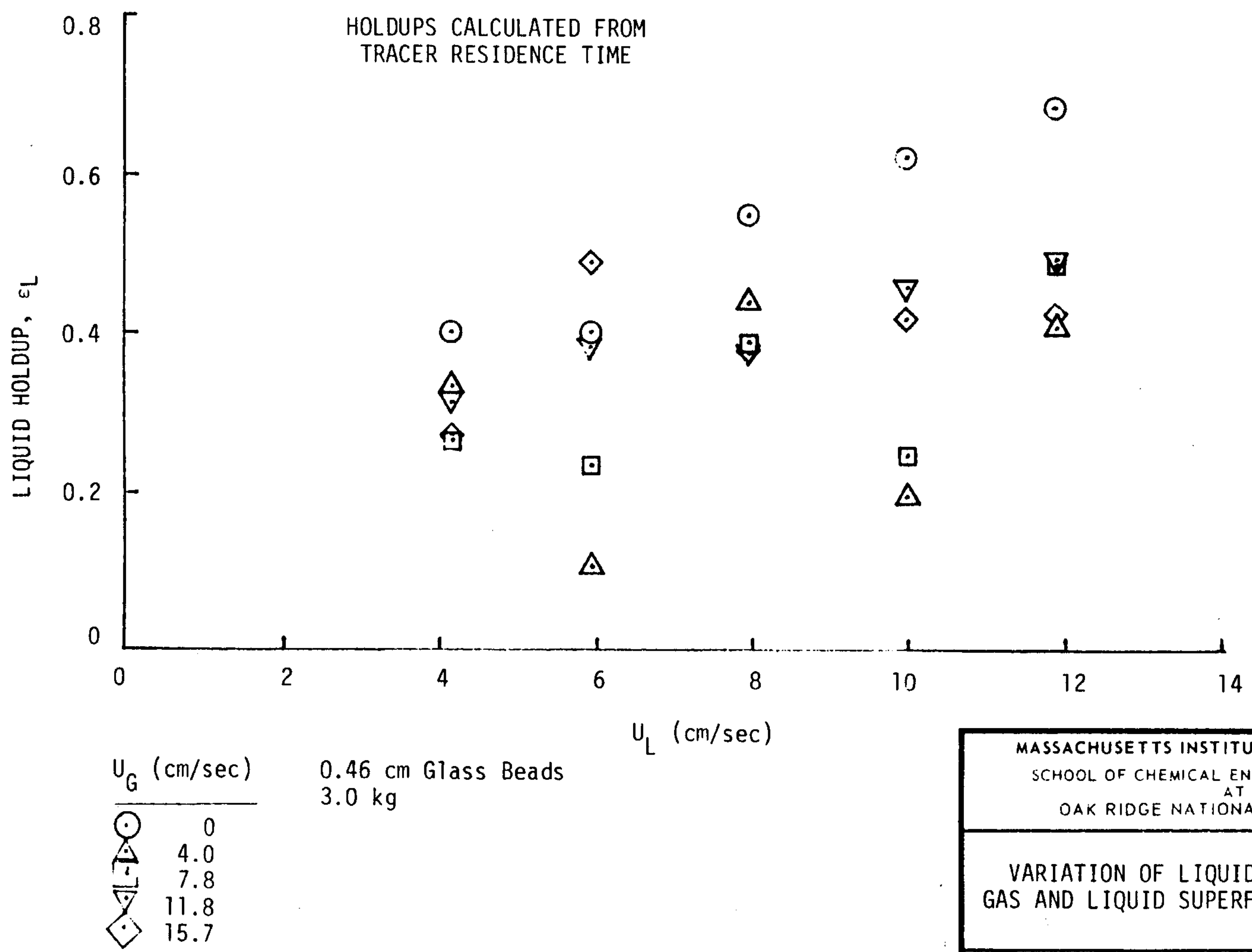

MASSACHUSETTS INSTITUTE OF TECHNOLOGY
SCHOOL OF CHEMICAL ENGINEERING PRACTICE
AT
OAK RIDGE NATIONAL LABORATORY

VARIATION OF LIQUID HOLDUP WITH GAS AND LIQUID SUPERFICIAL VELOCITY

DATE	DRAWN BY	FILE NO.	FIG.
4-21-77	ACS	CEP-X-254	5

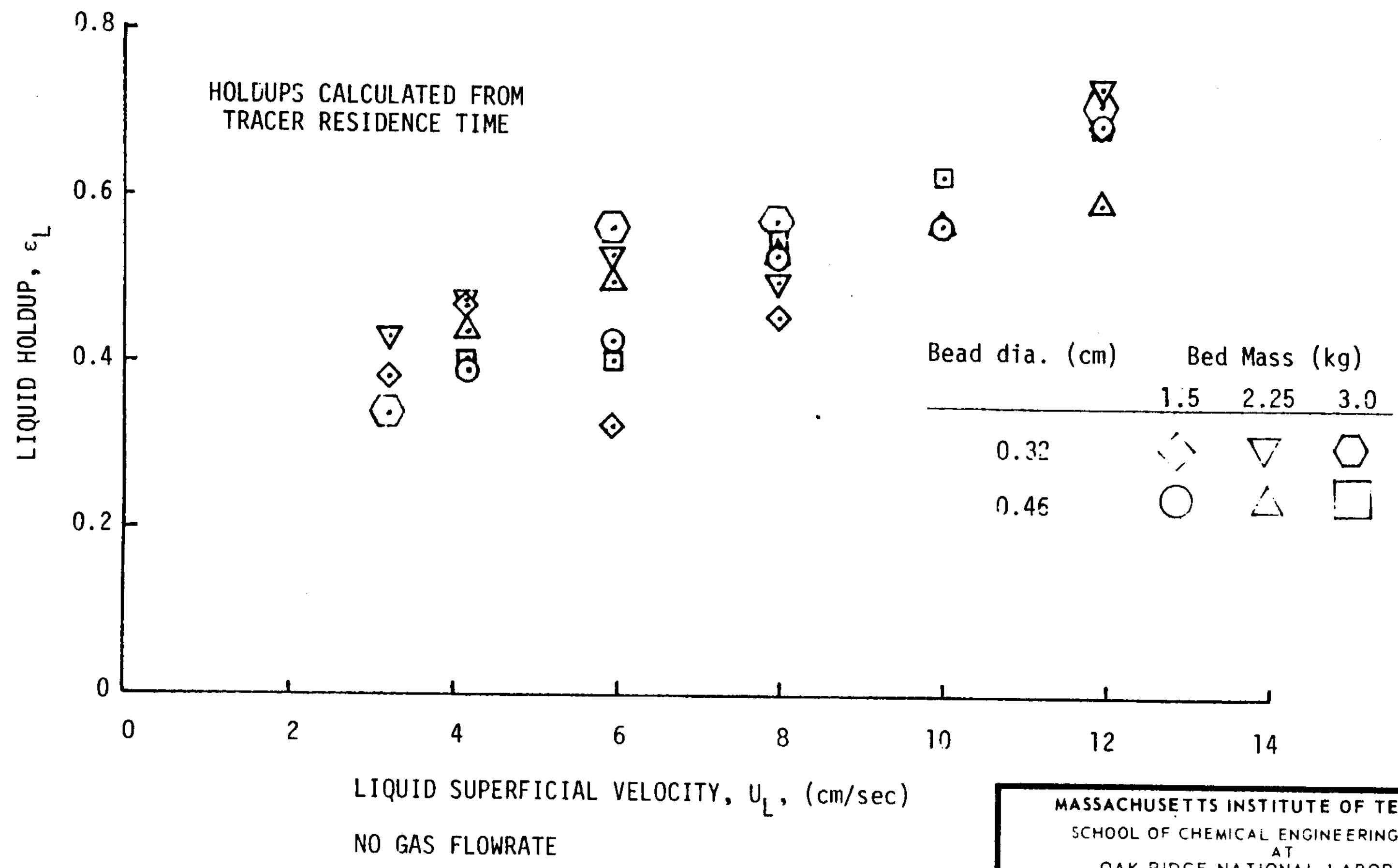

MASSACHUSETTS INSTITUTE OF TECHNOLOGY
SCHOOL OF CHEMICAL ENGINEERING PRACTICE
AT
OAK RIDGE NATIONAL LABORATORY

VARIATION OF LIQUID HOLDUP WITH SOLIDS LOADING AND PARTICLE DIAMETER

DATE	DRAWN BY	FILE NO.	FIG.
4/21/77	REB	CEP-X-254	6

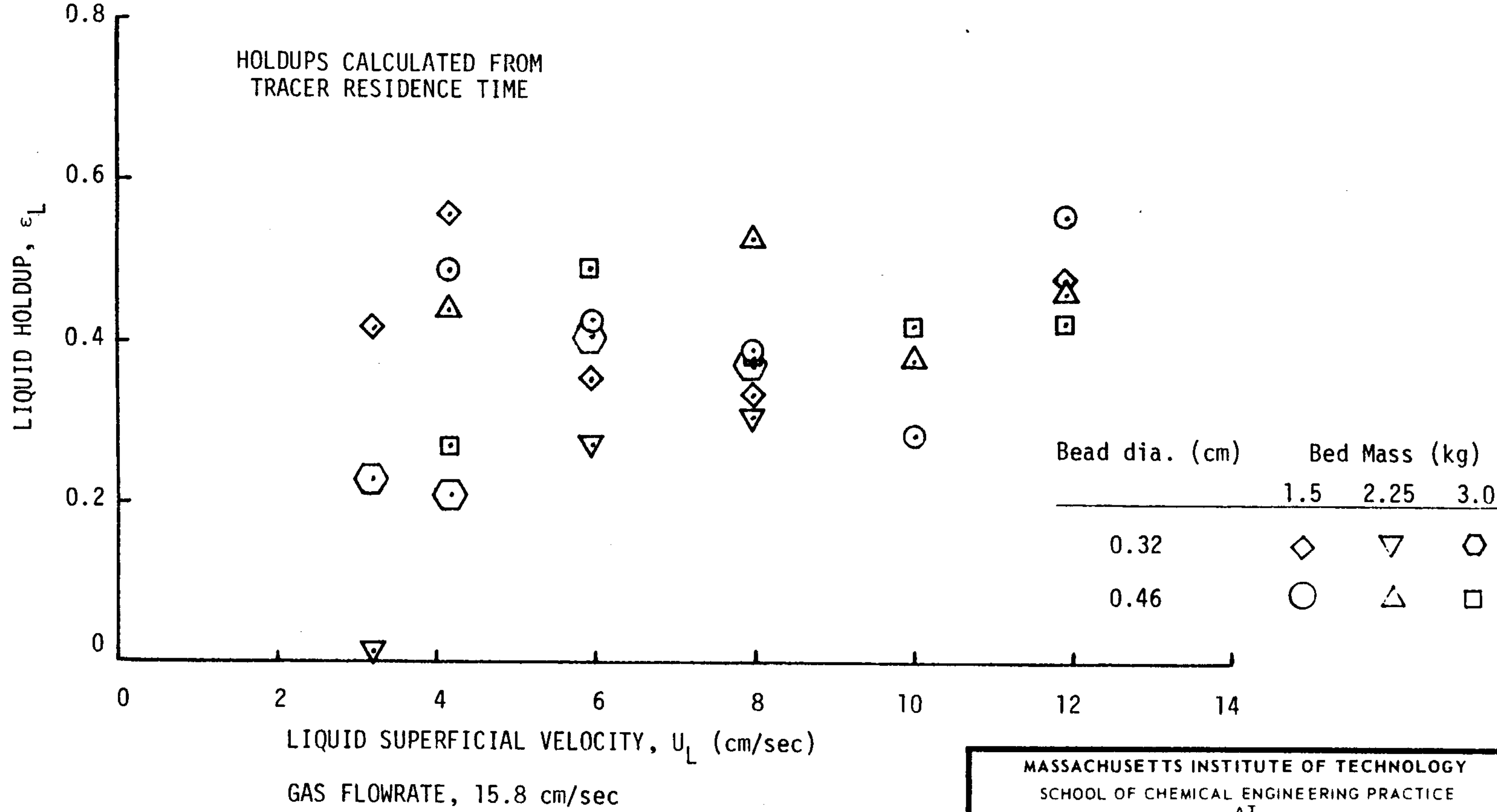

MASSACHUSETTS INSTITUTE OF TECHNOLOGY
SCHOOL OF CHEMICAL ENGINEERING PRACTICE
AT
OAK RIDGE NATIONAL LABORATORY

VARIATION OF LIQUID HOLDUP WITH SOLIDS LOADING AND PARTICLE DIAMETER

DATE	DRAWN BY	FILE NO.	FIG.
4-21-77	ACS	CEP-X-254	7

TABLE 2: DISPERSION COEFFICIENTS[1]

U_G (cm/sec)	U_L (cm/sec)	Method of Moments	Transfer Function	Modified Moments
0	4.2	4.68	-6.39	-27.5
	6.0	131	316	-3.94
	8.0	9.65	10.6	13.1
	10.0	11.0	10.5	9.82
	12.0	29.7	26.5	21.1
4.0	4.2	33.7	43.5	73.7
	6.0	2.91×10^3	3.93×10^3	-2.72
	8.0	766	1.71×10^3	-0.993
	10.0	125	362	108
	12.0	214	285	2310
7.9	4.2	91.3	107	7.31
	6.0	1.03×10^3	1.14×10^3	195
	8.0	219	282	476
	10.0	-216	408	3.39×10^3
	12.0	150	175	839
11.9	4.2	91.1	113	157
	6.0	278	386	505
	8.0	327	439	638
	10.0	167	181	205
	12.0	294	364	515
15.9	4.2	201	268	237
	6.0	168	266	685
	8.0	162	252	353
	10.0	142	187	357
	12.0	482	618	1.02×10^3

[1] 3 kg loading; 0.46-cm glass beads

TABLE 3: DISPERSION COEFFICIENTS[1]

U_G (cm/sec)	U_L (cm/sec)	Method of Moments	Transfer Function	Modified Moments
0	3.2	28.4	55.5	291
	4.2	-	-	-
	6.0	3.83	4.56	6.12
	8.0	9.66	12.8	22.3
	12.0	29.1	29.5	33.7
4.0	3.2	43.0	60.3	124
	4.2	2.47×10^4	-1.70×10^7	-5.75
	6.0	-3.59×10^3	7.55×10^3	1.44×10^{-3}
	8.0	216	237	197
	12.0	691	2.76×10^4	-2.79×10^5
7.9	3.2	150	271	1.01×10^{-4}
	4.2	-4.25×10^7	-8.84×10^4	0.113
	8.0	180	242	390
	12.0	139	144	156
11.9	3.2	690	1.35×10^3	-15.6
	4.2	-1.11×10^5	-2.07×10^4	-254
	6.0	44.4	-91.5	-168
	8.0	-5.51×10^3	-1.02×10^3	137
	12.0	-	-	-
15.9	3.2	297	385	161
	4.2	652	1.77×10^3	-99.7
	6.0	369	694	-577
	8.0	196	237	509
	12.0	-	-	-

[1] 3 kg loading; 0.32-cm glass beads

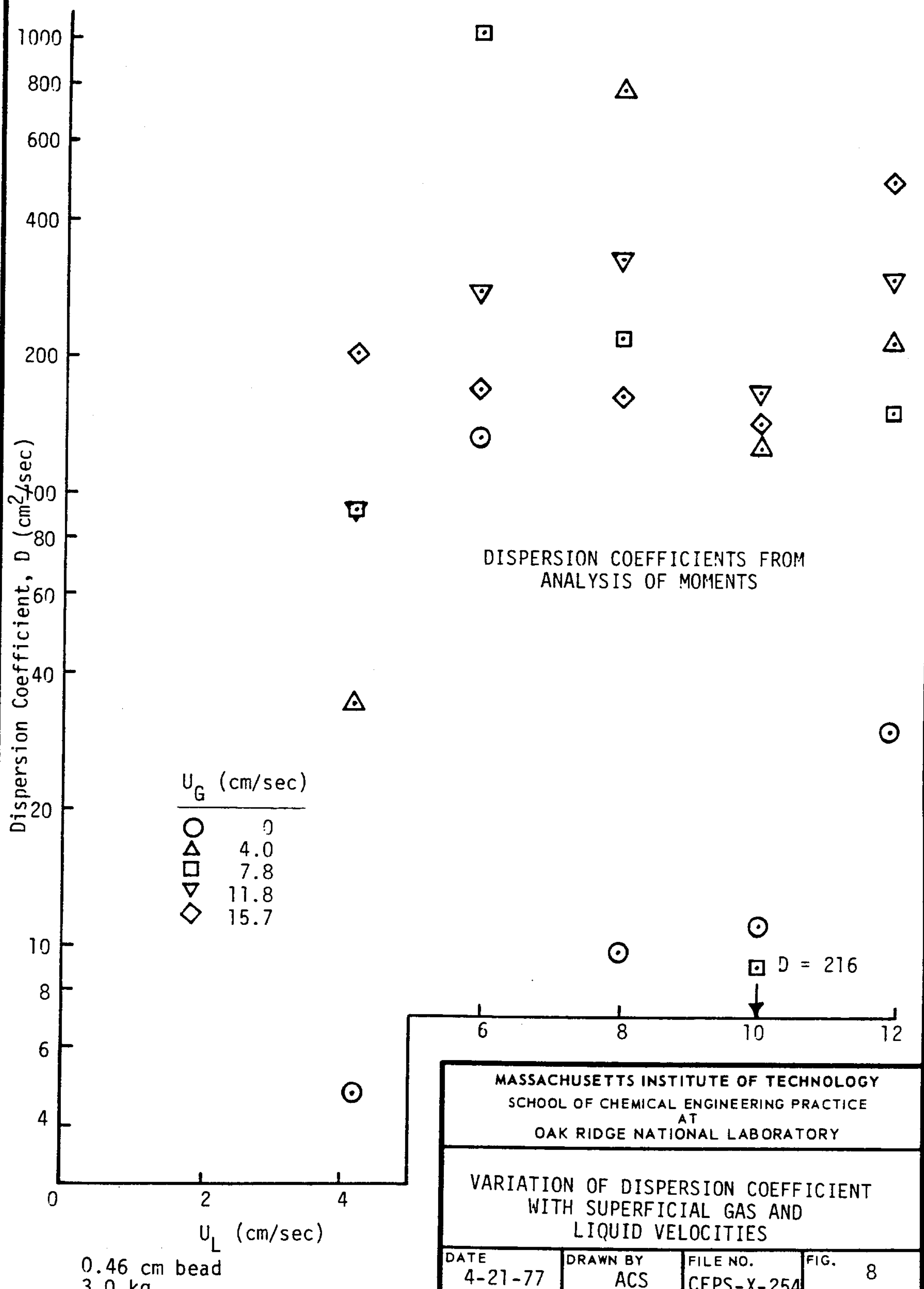

MASSACHUSETTS INSTITUTE OF TECHNOLOGY
SCHOOL OF CHEMICAL ENGINEERING PRACTICE
AT
OAK RIDGE NATIONAL LABORATORY

VARIATION OF DISPERSION COEFFICIENT WITH SUPERFICIAL GAS AND LIQUID VELOCITIES

DATE	DRAWN BY	FILE NO.	FIG.
4-21-77	ACS	CEPS-X-254	8

Figures 9 and 10 show the effect of varying particle size and solids loading on the dispersion coefficients at zero and maximum gas flowrates. Again, no relation among the variables is apparent.

5.3 Sources of Error

The wide variation in dispersion coefficients calculated by the three methods prompted a test of the methods with concentration data generated from a normal distribution function (8).

$$C(t) = \frac{1}{2\sqrt{\pi D t}} \exp\left[\frac{-(z - ut)^2}{4Dt}\right] \qquad (21)$$

The dispersion coefficients produced with such symmetric data are listed in Table 4. Several values of the transform variable s were used in this

TABLE 4: DISPERSION COEFFICIENTS CALCULATED WITH NORMAL DISTRIBUTION

Dispersion Coefficient (cm^2/sec)			
Moments	Modified Moments[1]	Transfer Function	s Range[2]
0.493	0.487	0.493	0.01 - 0.10
		0.491	0.08 - 0.42
		0.487	0.03 - 1.20
		0.485	1.10 - 2.00
		0.493	1.80 - 3.60
		0.541	3.60 - 5.40
		0.714	5.00 - 9.50

(1) S = 0.4
D = 0.5 in Eq. (21).

(2) Overflow errors occur for s > 36.

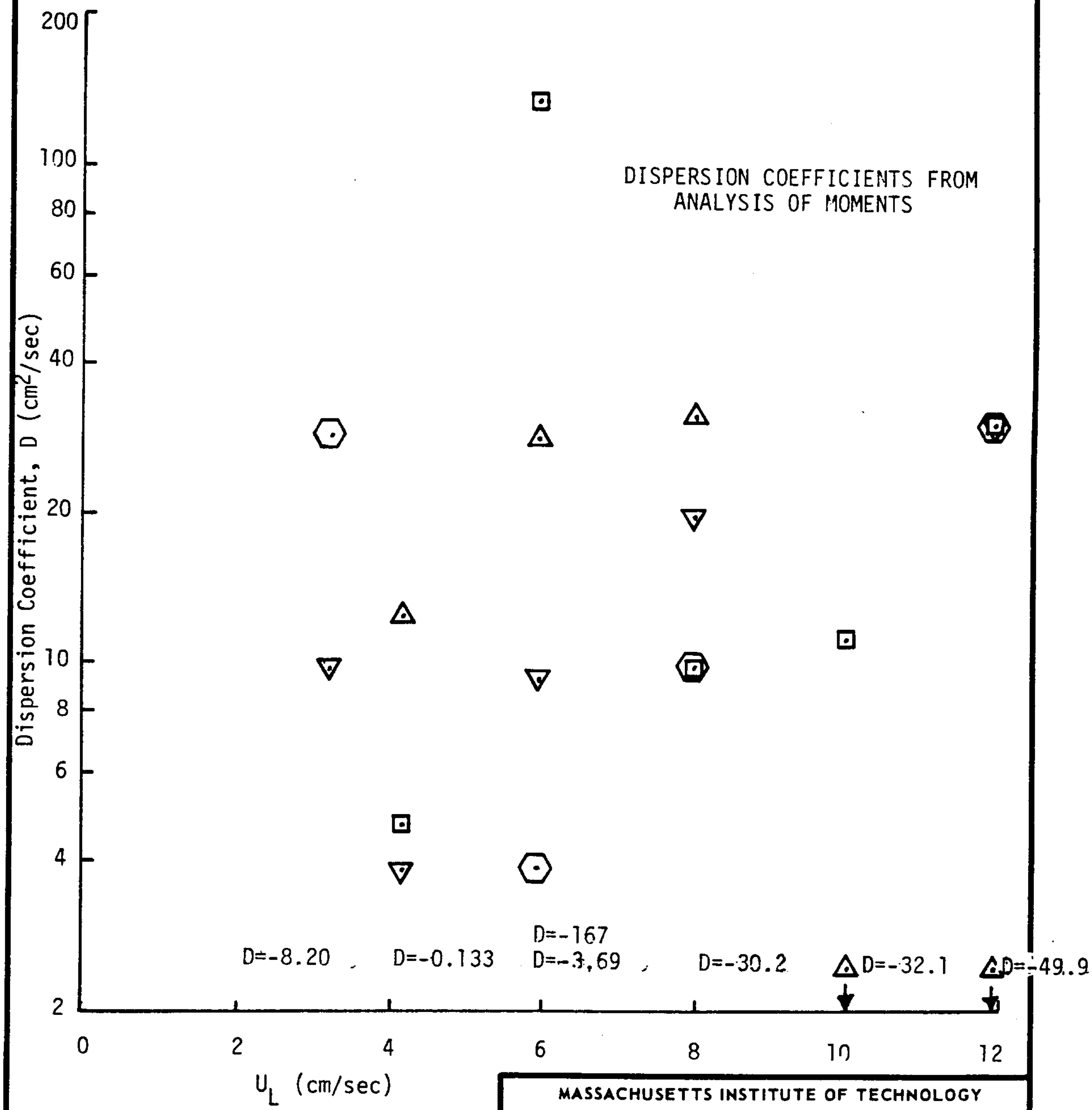

Bead dia. (cm)	Loading (kg) 2.25	3.0
0.32	▽	⬡
0.46	△	□

NO GAS FLOWRATE

MASSACHUSETTS INSTITUTE OF TECHNOLOGY
SCHOOL OF CHEMICAL ENGINEERING PRACTICE
AT
OAK RIDGE NATIONAL LABORATORY

VARIATION OF DISPERSION COEFFICIENT WITH SOLIDS LOADING AND PARTICLE DIAMETER

DATE	DRAWN BY	FILE NO.	FIG.
4-21-77	ACS	CEPS-X-254	9

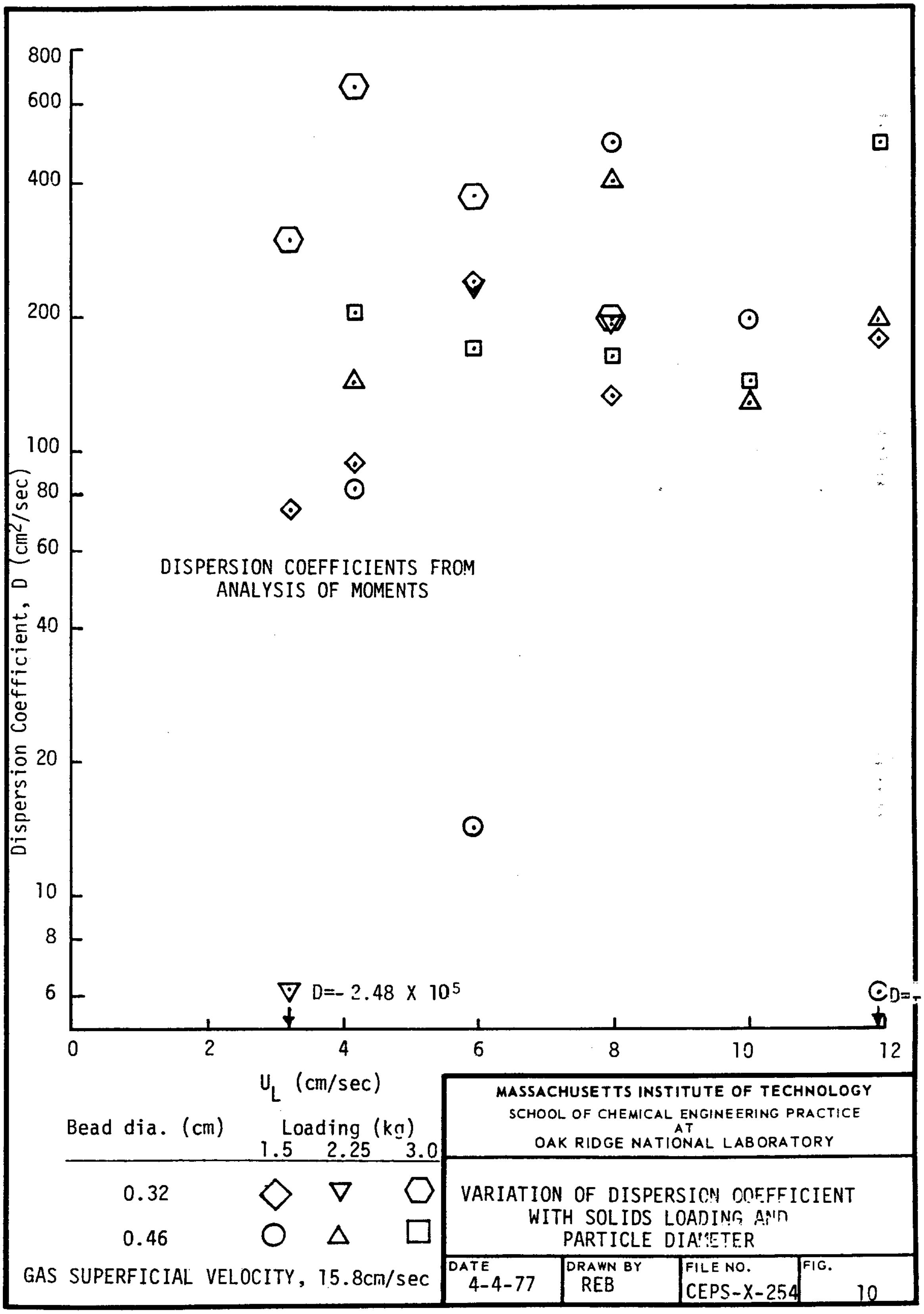
800
600
400
200
100
80
60
40
20
10
8
6
Dispersion Coefficient, D (cm²/sec)
DISPERSION COEFFICIENTS FROM
ANALYSIS OF MOMENTS
D=- 2.48 X 10⁵
D=-1226
0
2
4
6
8
10
12
U_L (cm/sec)
Bead dia. (cm)
Loading (kg)
1.5
2.25
3.0
0.32
0.46
GAS SUPERFICIAL VELOCITY, 15.8cm/sec
MASSACHUSETTS INSTITUTE OF TECHNOLOGY
SCHOOL OF CHEMICAL ENGINEERING PRACTICE
AT
OAK RIDGE NATIONAL LABORATORY
VARIATION OF DISPERSION COEFFICIENT
WITH SOLIDS LOADING AND
PARTICLE DIAMETER
DATE
4-4-77
DRAWN BY
REB
FILE NO.
CEPS-X-254
FIG.
10

simulation. There is better agreement among the transfer function and moments methods than with the experimental data. However, the choice of the transform variables affects this agreement with s values of 0.01 to 0.1 and 1.80 to 3.60 providing the closest match. This type of analysis should be repeated for a skewed distribution that would more accurately reflect the form of the experimental data. In addition to the errors associated with the computation of the dispersion coefficients, the uncertainty in the data base was also significant. The lack of reproducibility in the tracer measurements is illustrated in Fig. 11. The three sets of tracer concentration curves are the responses, at the first and second pair of electrodes, to identical tracer inputs. Two major problems that could account for the irreproducibility are large scale transients in the mixing within the column and cross-conductivity between the electrodes. Observations of bead movement within the column revealed that there were sudden upsurges, or swirls, of liquid and beads through the test section that would greatly affect the tracer distribution. Redesign of the gas and liquid distributors to provide more stable fluidization of the beads and locating the test section further from the fluid inlets should eliminate this part of the problem. The cross-conductivity between the two sets of electrodes was detected near the end of the project. As can be seen in Fig. 11, the second set of electrodes is responding to the tracer input during the same time span as the first set. The extent of this interaction between the electrodes was estimated by measuring the baseline conductivity of each pair of electrodes with a water-potassium chloride solution circulating through the column. Disconnecting one of the 110-volt, 3000-Hz conductivity meters decreased the solution conductivity measured at the other meter. This decrease was equivalent to a 35% reduction in peak height for the tracer concentration used throughout this investigation. Increasing the distance between the electrode sets decreased the cross-conductivity. The 35% interaction occurred with 8-cm spacing and this dropped to 10% at 30 cm and less than 1% at 42 cm. Only the dispersion coefficient experiments with 3 kg loadings had electrode spacings greater than 30 cm (Appendix 9.3).

Of all the experiments conducted, the most reproducible should have been those to determine the liquid holdup with no beads or gas in the column (Fig. 2). Table 5 lists the range of values and standard deviations for the hold-up calculated by the moments method at four liquid velocities. These data illustrate the difficulty of obtaining consistent results, even at large electrode spacings, with the present apparatus.

6. CONCLUSIONS

1. Calculated and experimentally determined liquid holdups in the liquid-only system are in good agreement for superficial liquid velocities greater than 6 cm/sec.

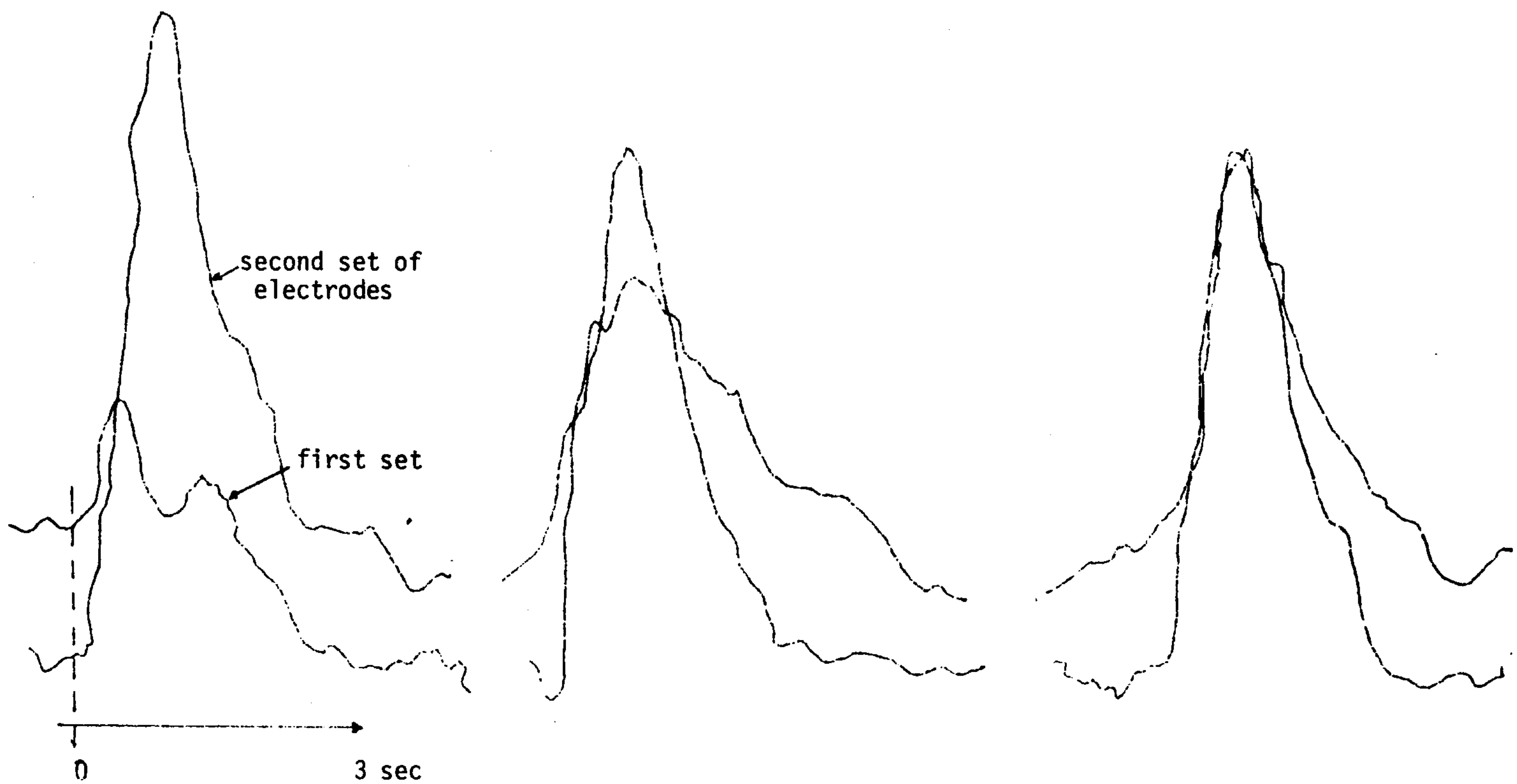

U_L = 11.9 cm/sec
U_G = 12.7 cm/sec
1.5 kg of 0.62 cm beads
Le = 8 cm

MASSACHUSETTS INSTITUTE OF TECHNOLOGY
SCHOOL OF CHEMICAL ENGINEERING PRACTICE
AT
OAK RIDGE NATIONAL LABORATORY

IRREPRODUCIBILITY OF TRACER RESPONSE

DATE	DRAWN BY	FILE NO.	FIG.
4/21/77	ACS	CEPS-X-254	11

TABLE 5: LIQUID HOLDUP VALUES FOR
NO SOLIDS OR GAS FLOW

Superficial Liquid Velocity (cm/sec)	Holdup (ε_L)	Mean	Standard Deviation
1.91	0.6708		
	0.5558		
	0.6285		
	1.0925		
		0.737	0.209
3.22	0.5533		
	0.5611		
	1.8467		
	1.0999		
		1.015	0.528
4.18	0.5268		
	1.5006		
	1.2099		
	1.1950		
	1.3365		
		1.154	0.332
5.96	1.0070		
	0.9631		
	1.8872		
		1.286	0.426

Electrode spacing was 36 cm for all experiments

2. The tracer tests did not yield statistically significant results for the dependence of the dispersion coefficient on particle size, mass loading, and superficial gas and liquid velocities because of transient mixing in the column and cross coupling between the conductivity meters.

3. Dispersion coefficients calculated with data for a normal distribution were essentially the same for the three methods of analysis.

7. RECOMMENDATIONS

1. Redesign the fluid distributors to achieve stable bed fluidization.

2. Raise the position of the test section in the column to eliminate entrance effects.

3. Limit further experiments to one loading and particle size so that holdups and the dispersion coefficient can be correlated with fluid velocities and the apparent drop in the dispersion coefficient at large liquid flowrates can be verified.

8. ACKNOWLEDGEMENTS

The advice and assistance of J.M. Begovich, J.S. Watson and S.D. Clinton throughout the project was greatly appreciated.

9. LOCATION OF DATA

Data for all experiments are located in notebook A-7556-G, p. 1-28, and program printouts for the analysis of these experiments are on file at the M.I.T. Practice School, Bldg. 3001, ORNL.

10. APPENDIX

10.1 Program Listing

TRACER,FTN

TABLE OF SYMBOLS

B1	BASELINE ORDINATE OF FIRST PEAK
B2	BASELINE ORDINATE OF SECOND PEAK
C	AVERAGE CONCENTRATION READING FOR THE TIME INTERVAL
CDELT	CONCENTRATION TIMES TIME INTERVAL
CDELT1	CONCENTRATION*TIME INTERVAL, FIRST PEAK
CHS	CHART SPEED (IN/MIN)
CONINT	95% CONFIDENCE INTERVAL FOR Y INTERCEPT
CPB	CONCENTRATION PLUS BASELINE (ABSOLUTE READING)
CS	INTEGRAL OF CONCENTRATION TIMES EXP(-ST)
CSA	CROSS SECTIONAL AREA OF COLUMN (SQ CM)
C1S	CS FOR THE FIRST PEAK
D	REAL LIQUID PHASE AXIAL DISPERSION COEFFICIENT (CM SQ/SEC)
DELH	DIFFERENCE OF MANOMETER READINGS THROUGH BED (CM H2O)
DELP	PRESSURE DROP THROUGH BED (CM H2O)
DELPHG	PRESSURE DROP THROUGH ENTIRE COLUMN, READ FROM HG MANOMETER (MM HG)
DELSIG	SIGSQ2 - SIGSQ1
DELTAT	TIME INTERVAL
DELTBR	(MEAN RESIDENCE TIME)2 - (MEAN RESIDENCE TIME)1
DENOM	DENOMINATOR FOR THE LEAST SQUARES SLOPE
DIA	COLUMN DIAMETER (CM)
DIMSIG	DIMENSIONLESS VARIANCE
DP	PARTICLE DIAMETER (CM)
DPTF	TRANSFER FUNCTION DISPERSION COEFFICIENT
EG	GAS VOLUME FRACTION WITH RESPECT TO TOTAL VOLUME
EGPTF	GAS VOLUME FRACTION - TRANSFER FUNCTION, TOTAL VOLUME
EL	LIQUID VOLUME FRACTION WITH RESPECT TO TOTAL VOLUME
ELPTF	LIQUID VOLUME FRACTION - TRANSFER FUNCTION, TOTAL VOLUME
E1G	GAS VOLUME FRACTION NOT USING MEAN RESIDENCE TIME
E1L	LIQUID VOLUME FRACTION NOT USING MEAN RESIDENCE TIME
E1S	SOLIDS VOLUME FRACTION NOT USING MEAN RESIDENCE TIME
F	TRANSFER FUNCTION F(S)
GASPER	GAS FLOW RATE (ROTAMETER SCALE READING)
H	BED HEIGHT (CM)
I	DO LOOP COUNTER
IRDGRT	I READ GAS RATE - GAS ROTAMETER NUMBER
IRDLRT	I READ LIQUID RATE - LIQUID ROTAMETER NUMBER
ITT	PEAK COUNTER (WORKING ON FIRST OR SECOND PEAK)
L	DISTANCE BETWEEN ELECTRODES (CM)
L1	CHARACTERS FOR NAMING OF DATA INPUT FILE
L2	CHARACTERS OF INPUT FILE NUMBER
M	TOTAL NUMBER OF CHARACTERS FOR DATA FILE NAME

MUG	GAS VISCOSITY (POISE)
MUL	LIQUID VISCOSITY (POISE)
NCONT	RESPONSE FOR DESIRE WHETHER TO CONTINUE
NO1	NUMBER OF POINTS IN FIRST PEAK
NO2	NUMBER OF POINTS IN SECOND PEAK
NRUN	RUN NUMBER
NU	NUMBER OF DIGITS IN NUMBER OF INPUT DATA FILE
NUM	NUMERATOR FOR LEAST SQUARES SLOPE
PATM	ATMOSPHERIC PRESSURE AT THE TIME OF THE RUN (MM HG)
PE	PECLET NUMBER (VL*L/D)
PEDP	PECLET NUMBER BASED ON PARTICLE DIAMETER
PEPTF	PECLET NUMBER FROM TRANSFER FUNCTION
PEPTFD	TRANSFER FUNCTION PECLET NUMBER BASED ON PARTICLE DIAMETER
PEPTFH	HIGH VALUE OF 95% CONFIDENCE INTERVAL
PEPTFL	LOW VALUE OF 95% CONFIDENCE INTERVAL
R	CORRELATION COEFFICIENT (LEAST SQUARES FIT)
REG	GAS REYNOLDS NUMBER BASED ON PARTICLE DIAMETER
REGPTF	GAS REYNOLDS NUMBER BASED ON PARTICLE DIAMETER (TRANSFER FUNCTION)
REGS	GAS REYNOLDS NUMBER USING SUPERFICIAL VELOCITY
REL	LIQUID REYNOLDS NUMBER BASED ON PARTICLE DIAMETER
RELPTF	LIQUID REYNOLDS NUMBER BASED ON PARTICLE DIAMETER (TRANSFER FUNCTION)
RELS	LIQUID REYNOLDS NUMBER USING SUPERFICIAL VELOCITY
RHOG	GAS DENSITY (GM/CC)
RHOL	LIQUID DENSITY (GM/CC)
RHOS	SOLID DENSITY (GM/CC)
RSQ	CORRELATION NUMBER IN LEAST SQUARES FIT (SQUARE OF R)
S	ARBITRARY NUMBERS FOR TRANSFER FUNCTION
SCEST	ACCUMULATOR FOR INTEGRATING LAPLACE TRANSFORM OF CONCENTRATION
SD	STANDARD DEVIATION (ACTUAL AND PREDICTED VALUES ON TRANSFER FUNCTION PLOT
SIGSQ	SIGMA SQUARED, VARIANCE
SIGSQ1	VARIANCE OF FIRST PEAK
SMASS	SOLIDS LOADING (GRAMS)
SUMC	INTEGRAL OF CONCENTRATION
SUMDIF	SUM OF SQUARED DIFFERENCES FOR SD
SUMTC	INTEGRAL OF C*TIME (FIRST MOMENT)
SUMTTC	INTEGRAL OF C*TIME SQUARED (SECOND MOMENT)
SUMX	SUM OF X TO FIND XMEAN IN LEAST SQUARES FIT
SUMXX	SUM OF X SQUARED TO FIND VARIANCE OF X
SUMXY	SUM OF X*Y FOR COVARIANCE
SUMY	SUM OF Y TO FIND YMEAN
SUMYY	SUM OF Y SQUARED TO FIND VARIANCE OF Y
T	ABSCISSA OF PEAK IN CHART SQUARES (10 SQUARES/IN)

TAU	SLOPE OF TRANSFER FUNCTION PLOT, MEAN RESIDENCE TIME
TAVG	MIDPOINT OF TIME INTERVAL
TBAR	MEAN RESIDENCE TIME , SECOND PEAK
TBAR1	FIRST PEAK
TEMP	LIQUID TEMPERATURE (DEG C)
TM	AVERAGE TIME IN CHART SQUARES
TMEAN	AVERAGE TIME IN SECONDS
V	LIQUID FLOW RATE (ROTAMETER SCALE READING)
VDN	LIQUID PHASE AXIAL DISPERSION NUMBER
VDNPTF	DISPERSION NUMBER FROM TRANSFER FUNCTION
VG	REAL GAS VELOCITY (CM/SEC)
VGPTF	GAS INTERSTITIAL VELOCITY BASED ON TRANSFER FUNCTION CALCULATION (CM?SEC)
VGSUP	SUPERFICIAL GAS VELOCITY (CM/SEC).
VGSUPV	SUPERFICIAL GAS FLOW RATE (CC/SEC)
VL	REAL LIQUID VELOCITY (CM/SEC)
VLSUP	SUPERFICIAL LIQUID VELOCITY (CM/SEC)
VLSUPV	SUPERFICIAL LIQUID FLOW RATE (CC/SEC)
VLPTF	LIQUID INTERSTITIAL VELOCITY BASED ON TRANSFER FUNCTION CALCULATION (CM/SEC)
X	ABSCISSA OF TRANSFER FUNCTION POINTS
Y	ORDINATE OF TRANSFER FUNCTION POINTS
YINT	Y INTERCEPT OF TRANSFER FUNCTION PLOT
YINTH	HIGH VALUE OF 95% CONFIDENCE INTERVAL
YINTL	LOW VALUE OF 95% CONFIDENCE INTERVAL
YPRED	VALUE PREDICTED FOR Y BY LEAST SQUARES SLOPE AND INTERCEPT

```
      REAL L,MUG,MUL,NUM
      DIMENSION CPB(120),CDELT(120),TAVG1(120),TAVG(120),
     $  T(120),S(10),CS(10),C1S(10),F(10),X(10),Y(10),
     $  TAVGX(120),SCEST(10),CDELTX(120),CDELT1(120)
      DATA DIA/7.62/,
     $S/.08531,.09,.13438,.12,.13918,.17,.20876,.27,.34,.41783/
      CSA = DIA*DIA*0.785398
      J=30
5     J=J+1
10    ITT =1
      READ (J,300,END=100) NRUN, NO1, NO2, B1, B2, V, GASPER,
     *   DELPHG, PATM, CHS
      READ (J,31) DP, RHOS, TEMP, L, H, DELH, SMASS
      READ (J,32) IROGRT, IRDLRT
      GO TO (11,12,11,11,11,13,11), IROGRT
 11   TYPE 14, IROGRT, NRUN
      GO TO 10
 12   VGSUPV = GASPER*0.53333*SQRT(749.8/(PATM+DELPHG))
      GO TO 16
 13   VGSUPV = GASPER*8.5526*SQRT(749.8/(PATM+DELPHG))
 16   VGSUP = VGSUPV/CSA
      GO TO (18,19,20,17,21,17), IRDLRT
 17   TYPE 22, IRDLRT, NRUN
      GO TO 10
 18   VLSUPV = V*5.44
      GO TO 23
 19   VLSUPV = V*0.323
      GO TO 23
 20   VLSUPV = V*13.383
      GO TO 23
 21   VLSUPV = V*2.79
 23   VLSUP = VLSUPV/CSA
      MUL = (1.3508 - 0.017445*TEMP)*0.01
      MUG = (0.01718 + 0.0000475*TEMP)*0.01
      RHOL = 1.00401 - 0.00028*TEMP
      DELP = (DELH*H)*RHOL/1.356
      RHOG = 0.0004626*(PATM+DELPHG-0.5*DELP)/(273.15+TEMP)
      TMEAN = L/VLSUP
 25   CONTINUE
      IF(ITT.EQ.2) NO1 = NO2
      READ(J,350) (T(I),CPB(I),I=1,NO1)
      IF(ITT .EQ. 1) GO TO 30
      DO 35 I=1,NO1
 35   T(I)=T(I)-2.
 30   DO 42 I=1,NO1
 42   T(I) = T(I)*6.0/CHS
      SUMC = 0.0
      SUMTC = 0.0
      SUMTTC = 0.0
      DO 45 J=1,10
 45   SCEST(J) =0.0
      IF(ITT.EQ.2) B1 = B2
      CPB(1)=CPB(1)-B1
      DO 50 I = 2, NO1
      DELTAT = T(I) - T(I-1)
      CPB(I) = CPB(I) - B1
      C = (CPB(I)+CPB(I-1))/2.
      TAVG(I) = (T(I)+T(I-1))/2.
      CDELT(I) = C*DELTAT
      SUMC = SUMC + CDELT(I)
```

```
      SUMTC = SUMTC + CDELT(I)*TAVG(I)
      DO 54 J=1,10
54    SCEST(J) = SCEST(J) + CDELT(I)*EXP(-S(J)*TAVG(I))
50    CONTINUE
      TBAR = SUMTC/SUMC
      DO 52 I = 2, NO1
      SUMTTC = SUMTTC + CDELT(I)*(TAVG(I)-TBAR)*(TAVG(I)-TBAR)
52    CONTINUE
      DO 56 J=1,10
56    CS(J) = SCEST(J)/SUMC
      SIGSQ = SUMTTC/SUMC
      IF(ITT.EQ.2) GO TO 60
      DO 57 I=2,NO1
      CDELT1(I)=CDELT(I)
57    TAVG1(I)=TAVG(I)
      NO11=NO1
      TBAR1 = TBAR
      SIGSQ1 = SIGSQ
      DO 51 I = 1, 10
51    C1S(I) = CS(I)
      ITT = 2
      GO TO 25
60    DELSIG = SIGSQ - SIGSQ1
      DELTBR = TBAR - TBAR1
      E1S = SMASS/H/CSA/RHOS
      E1G = (DELH*RHOL/H - E1S*(RHOS-RHOL))/(RHOG - RHOL)
      E1L = 1.0 - E1S - E1G
      EL = DELTBR/TMEAN
      EG = ((DELH+H)*RHOL/H - EL*(RHOL-RHOS) - RHOS)/(RHOG - RHOS)
      DIMSIG = DELSIG/(DELTBR*DELTBR)
      VDN = DIMSIG/2.
      PE = 1.0/VDN
      VL = VLSUP/EL
      VG = VGSUP/EG
      REG = RHOG*DP*VG/MUG
      REGS = RHOG*DP*VGSUP/MUG
      REL = RHOL*DP*VL/MUL
      RELS = RHOL*DP*VLSUP/MUL
      PEDP = PE*DP/L
      D = VL*L*VDN
      DO 61 I = 1, 10
      F(I) = CS(I)/C1S(I)
      Y(I) = -1.0/ALOG(F(I))
61    X(I) = S(I)/(ALOG(F(I))*ALOG(F(I)))
      SUMX = 0.0
      SUMY = 0.0
      SUMXX = 0.0
      SUMXY = 0.0
      SUMYY = 0.0
      DO 62 I = 1,10
      SUMX = SUMX + X(I)
      SUMY = SUMY + Y(I)
      SUMXX = SUMXX + X(I)*X(I)
      SUMXY = SUMXY + X(I)*Y(I)
62    SUMYY = SUMYY + Y(I)*Y(I)
      NUM = SUMXY - (SUMX*SUMY/10.)
      DENOM = SUMXX - (SUMX*SUMX/10.)
      TAU = NUM/DENOM
      YINT = (SUMY-TAU*SUMX)/10.0
      SUMDIF = 0.0
```

```
      DO 63 I = 1, 10
      YPRED = YINT + TAU*X(I)
 63   SUMDIF = SUMDIF + (YPRED-Y(I))*(YPRED-Y(I))
      SD = SQRT(SUMDIF/8.)
      CONINT = SQRT(SUMXX/10.0/DENOM)*SD*2.306
      YINTH = YINT - CONINT
      YINTL = YINT + CONINT
      RSQ = NUM*NUM/((SUMXX-(SUMX*SUMX)/10.0)*(SUMYY-(SUMY*SUMY)/10.0))
      R = SQRT(RSQ)
      ELPTF = TAU/TMEAN
      EGPTF = ((DELH+H)*RHOL/H - ELPTF*(RHOL-RHOS) - RHOS)/(RHOG - RHOS)
      VLPTF = VLSUP/ELPTF
      VGPTF = VGSUP/EGPTF
      VDNPTF = -YINT
      PEPTF = -1.0/YINT
      PEPTFH = -1.0/YINTL
      PEPTFL = -1.0/YINTH
      PEPTFD = PEPTF*DP/L
      DPTF = VLPTF*L*VDNPTF
      RELPTF = RHOL*DP*VLPTF/MUL
      REGPTF = RHOG*DP*VGPTF/MUG
      SS=0.2
      ITT=1
      NOX=NO11
      DO 65 II=1,8
      DO 644 J=1,NOX
      CDELTX(J)=CDELT1(J)
644   TAVGX(J)=TAVG1(J)
64    SCEST0=0.0
      SCEST1 = 0.0
      SCEST2 = 0.0
      DO 66 I=2,NOX
      SCEST0 = SCEST0 + CDELTX(I)*EXP(-SS*TAVGX(I))
      SCEST1 = SCEST1 + TAVGX(I)*CDELTX(I)*EXP(-SS*TAVGX(I))
66    CONTINUE
      TBARS = SCEST1/SCEST0
      DO 68 I=2,NOX
      SCEST2 = SCEST2 + (TAVGX(I)-TBARS)**2.*CDELTX(I)*
     *  EXP(-SS*TAVGX(I))
68    CONTINUE
      IF(ITT .EQ. 2)GO TO 699
      DO 67 J=1,NO1
      CDELTX(J)=CDELT(J)
67    TAVGX(J)=TAVG(J)
      ITT=2
      NOX=NO1
      TBARS1 = TBARS
      SC21 = SCEST2/SCEST0
      GO TO 64
699   SSOLD=SS
      A=TBARS-TBARS1
      B=SCEST2/SCEST0 - SC21
      STAU=A*(1.-2.*SS*B/A)**-0.5
      IF(SS*STAU .LT. 0.9) SS=SS*2.
      IF(SS*STAU .GT. 2.5) SS=SS/2.
      IF(SSOLD .EQ. SS) GO TO 700
      ITT=1
      NOX=NO11
65    CONTINUE
700   CONTINUE
```

```
      SPE=2.*A**2./B*(1.-2.*B*SS/A)**0.5
      SPEDP=SPE*DP/L
      TYPE 69, NRUN
      PRINT 70, NRUN, VGSUPV, VGSUP, REGS, VLSUPV, VLSUP, RELS,
     *  TMEAN, E1G, E1L
      PRINT 71, VG, VL, REG, REL, TBAR1, TBAR, DELTBR, EG, EL,
     *  VDN, PE, PEDP, D
      PRINT 72, VGPTF, VLPTF, REGPTF, RELPTF, TAU, EGPTF, ELPTF,
     *  VDNPTF, PEPTF, PEPTFH, PEPTFL, PEPTFD, DPTF
      PRINT 722, STAU,SPE,SPEDP,SS
722   FORMAT(//,10X,' BY MODIFIED ANALYSIS OF MOMENTS',//,
     *12X,' RESIDENCE TIME ',F20.4,/,
     *12X, ' PECLET NUMBER ',F21.4,/,
     *12X,' PECLET NUMBER W,R,T. DP',F12.4,/,
     *12X,' TRANSFORM PARAMETER S',F14.4)
      PRINT 73
      PRINT 74, (S(I),C1S(I),CS(I),F(I),X(I),Y(I),I=1,10)
      PRINT 75,R
      GO TO 10
100   TYPE 111
111   FORMAT(///,' DO YOU WISH TO CONTINUE? YES OR NO',/)
      ACCEPT 112,ANSR
112   FORMAT(A3)
      IF(ANSR .EQ. 'YES') GO TO 5
 99   STOP
 300  FORMAT(10G)
 31   FORMAT (7G)
 32   FORMAT (2G)
 350  FORMAT (1(1X,F5.1,9(2X,F5.1)))
 69   FORMAT (5X,'RUN',I4)
 70   FORMAT (28X,'RUN NUMBER',I4//
     *  12X,'GAS FLOW RATE',F23.4,'  CC/SEC'/
     *  12X,'SUPERFICIAL GAS VELOCITY',F12.4,'  CM/SEC'/
     *  12X,'SUP. GAS REYNOLDS NO.',F15.4,/
     *  12X,'LIQUID FLOW RATE',F20.4,'  CC/SEC'/
     *  12X,'SUPERFICIAL LIQUID VELOCITY',F9.4,'  CM/SEC'/
     *  12X,'SUP. LIQUID REYNOLDS NO.',F12.4/
     *  12X,'LIQUID SPACE TIME'/
     *  12X,' (NEGLECTING GAS PRESENCE)',F10.4,'  SEC'/
     *  12X,'HOLDUPS NOT USING MEAN RESIDENCE TIME'/
     *  12X,' GAS',F32.4/
     *  12X,' LIQUID',F29.4//)
 71   FORMAT (24X,'BY ANALYSIS OF MOMENTS'//
     *  12X,'GAS VELOCITY',F24.4,'  CM/SEC'/
     *  12X,'LIQUID VELOCITY',F21.4,'  CM/SEC'/
     *  12X,'GAS REYNOLDS NO.',F20.4/
     *  12X,'LIQUID REYNOLDS NO.',F17.4/
     *  12X,'T BAR IN',F28.4,'  SECONDS'/
     *  12X,'T BAR OUT',F27.4,'  SECONDS'/
     *  12X,'MEAN LIQUID RESIDENCE TIME',F10.4,'  SECONDS'/
     *  12X,'GAS HOLDUP',F26.4/
     *  12X,'LIQUID HOLDUP',F23.4/
     *  12X,'VESSEL DISPERSION NO.',F15.4/
     *  12X,'PECLET NO.',F26.4/
     *  12X,'PECLET NO. W,R,T, DP',F16.4/
     *  12X,'AXIAL DISP. COEFF.',F18.4,'  CM SQ/SEC',///)
 72   FORMAT (18X,'BY EVALUATION OF TRANSFER FUNCTION'//
     *  12X,'GAS VELOCITY',F24.4,'  CM/SEC'/
     *  12X,'LIQUID VELOCITY',F21.4,'  CM/SEC'/
     *  12X,'GAS REYNOLDS NO.',F20.4/
```

```
     *  12X,'LIQUID REYNOLDS NO.',F17.4/
     *  12X,'MEAN LIQUID RESIDENCE TIME',F10.4,'  SECONDS'/
     *  12X,'GAS HOLDUP',F26.4/
     *  12X,'LIQUID HOLDUP',F23.4/
     *  12X,'VESSEL DISPERSION NO.',F15.4/
     *  12X,'PECLET NO.',F26.4/
     *  12X,'95% CONFIDENCE INTERVAL'/
     *  12X,' HIGH VALUE',F25.4/
     *  12X,' LOW VALUE',F26.4/
     *  12X,'PECLET NO. W.R.T. DP',F16.4/
     *  12X,'AXIAL DISP. COEFF.',F18.4,'  CM SQ/SEC')
73    FORMAT (//,6X,'S',9X,'C1(S)',7X,'C2(S)',8X,'F(S)',
     *  6X,'ABSCISSA',4X,'ORDINATE'/)
74    FORMAT (1X,E11.4,5E12.4)
75    FORMAT (1X,/,12X,'CORRELATION COEFFICIENT',F13.4,///)
14    FORMAT (' DID YOU REALLY USE ROTAMETER G',I1,' FOR RUN',I4,'?',/)
22    FORMAT (' DID YOU REALLY USE ROTAMETER L',I1,' FOR RUN',I4,'?',/)
95    FORMAT (I2)
      END
```

10.2 Tabulation of Operating Conditions, Dispersion Coefficients, and Holdups

Bead Diam (cm)	Mass	U_L	U_G	ε_G	ε_L[1]	D	L_e	Run
0.46	1.5	4.18	0	0.057	0.344			1
				0.032	0.388	9.72	8.3	
			4.39	0.108	0.338			2
				0.150	0.261	-327		
			7.91	0.145	0.311			3
				0.240	0.140	925		
			11.95	0.184	0.271			4
				0.160	0.316	101		
			15.93	0.214	0.280			5
				0.099	0.486	81.7		
		5.96	0	-0.007	0.517			6
				0.045	0.424	-3.69		
			4.03	0.050	0.426			7
				0.408	-2.19	3149		
			7.90	0.131	0.362			8
				0.412	-0.144	5021		
			11.93	0.136	0.391			9
				0.260	0.167	698		
			15.94	0.149	0.406			10
				0.140	0.422	14.1		
		7.99	0	-0.013	0.539			11
				-0.003	0.522	-30.23	12.7	
			7.86	0.115	0.440			13
				0.067	0.527	204		
			11.86	0.154	0.469			14
				0.127	0.517	451		
			15.89	0.169	0.445			15
				0.201	0.387	486		
		10.02	0	-0.003	0.589			16
				0.011	0.564	3.10	16.0	
			4.01	0.082	0.541			17
				0.103	0.503	257		
			7.85	0.104	0.551			18
				0.343	0.121	233		
			11.84	0.146	0.520			19
				0.398	0.066	-1.73×10^{5}		
			15.79	0.194	0.469			20
				0.298	0.281	195		

[1] First row holdups by bed height, second row by tracer.

Bead Diam (cm)	Mass	U_L	U_G	ε_G	ε_L	D	L_e	Run
0.46	1.5	11.93	0	-0.002	0.635			21
				-0.031	0.687	6.76	20.5	
			4.02	0.098	0.589			22
				-0.081	0.913	140		
			7.87	0.131	0.569			23
				0.160	0.518	146		
			11.88	0.162	0.556			24
				0.210	0.469	104		
			15.84	0.326	0.280			25
				0.174	0.554	-1226		
	2.25	4.18	0	0.115	0.290			26
				0.034	0.436	12.2	19.5	
			4.02	0.091	0.330			27
				0.100	0.312	21.0		
			7.87	0.135	0.307			28
				0.120	0.335	36.7		
			11.90	0.124	0.358			29
				0.148	0.314	137		
			15.86	0.119	0.360			30
				0.075	0.440	141		
		5.96	0	0.028	0.435			31
				-0.006	0.496	27.8	22.5	
			4.02	0.066	0.403			32
				0.404	-0.205	1279		
			7.87	0.115	0.373			33
				0.111	0.381	89.2		
			11.88	0.145	0.381			34
				0.203	0.278	329		
		7.99	0	-0.003	0.530			36
				-0.001	0.526	30.6	27	
			4.02	0.074	0.467			37
				0.016	0.572	144		
			7.86	0.114	0.441			38
				0.231	0.230	-248		
			11.87	0.150	0.434			39
				0.085	0.552	264		
			15.82	-0.023	0.622			40
				0.033	0.522	396		
		10.02	0	-0.001	0.581			41
				0.008	0.564	-32.1	32	
			4.02	0.061	0.559			42
				0.212	0.287	-1276		
			7.86	0.125	0.520			43
				0.215	0.357	922		
			11.84	0.154	0.499			44
				0.200	0.416	222		
			15.79	0.186	0.475			45
				0.242	0.373	126		

Bead Diam (cm)	Mass	U_L	U_G	ε_G	ε_L	D	L_e	Run
0.46	2.25	11.93	0	0.004	0.632			46
				0.027	0.590	-49.9	32	
			4.02	0.094	0.608			47
				0.390	0.075	96,220		
			7.87	0.133	0.515			48
				0.192	0.469	435		
			11.87	0.177	0.533			49
				0.310	0.294	1373		
			15.81	0.192	0.537			50
				0.236	0.458	194		
	3	4.18	0	-0.026	0.374			51
				-0.041	0.401	4.685	26.5	
			4.01	0.095	0.323			52
				0.089	0.334	33.7		
			7.85	0.132	0.313			53
				0.161	0.261	91.3		
			11.84	0.159	0.292			54
				0.148	0.311	91.1		
			15.81	0.177	0.289			55
				0.187	0.270	201		
		5.96	0	-0.007	0.458			56
				0.026	0.399	131		
			3.96	0.080	0.386			57
				0.236	0.105	2914		
			7.75	0.120	0.365			58
				0.194	0.231	1026		
			11.69	0.139	0.372			59
				0.134	0.381	278		
			15.61	0.172	0.369			60
				0.106	0.488	168		
		7.99	0	0.004	0.515			61
				-0.014	0.547	9.65	35.5	
			4.01	0.073	0.475			62
				0.093	0.438	766		
			7.84	0.109	0.445			63
				0.142	0.387	219		
			11.82	0.142	0.419			64
				0.164	0.379	327		
			15.76	0.182	0.410			65
				0.199	0.380	162		
		10.02	0	-0.005	0.586			66
				-0.025	0.621	11.0	42	
			4.00	0.095	0.523			67
				0.279	0.193	125		
			7.84	0.131	0.506			68
				0.276	0.245	-216		

Bead Diam (cm)	Mass	U_L	U_G	ε_G	ε_L	D	L_e	Run
0.46	3	10.02	11.82	0.146	0.502			69
				0.171	0.457	167	42	
			15.74	0.190	0.474			70
				0.221	0.418	142		
		11.93	0	-0.003	0.641			71
				-0.027	0.684	29.7	48	
			4.00	0.099	0.595			72
				0.205	0.404	214		
			7.83	0.134	0.563			73
				0.177	0.485	150		
			11.79	0.175	0.536			74
				0.200	0.490	294		
			15.72	0.216	0.500			75
				0.261	0.420	482		
0.32	1.5	3.22	0	0.048	0.364			76
				0.039	0.381	-8.20	7	
			4.04	0.123	0.333			77
				0.220	0.158	104		
			7.91	0.135	0.359			78
				0.148	0.334	57.1		
			11.95	0.136	0.390			79
				0.221	0.237	10.91		
			15.94	0.187	0.323			80
				0.137	0.414	73.5		
		4.18	0	0.078	0.378			81
				0.029	0.467	-0.133	9.5	
			4.04	0.011	0.455			82
				0.177	0.155	1186		
			7.91	0.109	0.410			83
				0.321	0.027	-9.09×10^5		
			11.94	0.116	0.397			84
				0.172	0.298	249		
			15.93	0.150	0.391			85
				0.059	0.555	91.9		
		5.96	0	0.013	0.541			86
				0.127	0.322	-167		
			4.04	0.060	0.450			87
				0.089	0.399	23.7		
			7.90	0.107	0.419			88
				0.431	-0.164	368		
			11.94	0.154	0.394			89
				0.313	0.108	-7496		
			15.98	0.157	0.391			90
				0.180	0.351	237		

Bead Diam (cm)	Mass	U_L	U_G	ε_G	ε_L	D	L_e	Run
0.32	1.5	7.99	0	0.005	0.618			91
				0.098	0.451	276	14.5	
			4.04	0.079	0.524			92
				-0.006	0.677	125		
			7.90	0.100	0.513			93
				0.191	0.349	123		
			11.92	0.115	0.493			94
				0.152	0.427	210		
			15.91	0.159	0.483			95
				0.243	0.331	131		
		11.93	0	0.010	0.702			96
				0.022	0.680	3.49	26	
			4.04	0.092	0.678			97
				0.211	0.465	277		
			7.90	0.118	0.659			98
				0.389	0.172	-1.03×10^4		
			11.91	0.159	0.622			99
				-0.491	1.792	34.9		
			15.88	0.218	0.547			100
				0.258	0.475	173		
	2.25	3.22	0	0.024	0.373			101
				-0.008	0.429	9.64	18.5	
			4.03	0.631	0.312			102
				0.546	0.402	43.2		
			7.89	0.149	0.300			103
				0.063	0.455	49.3		
			15.87	0.199	0.257			105
				0.335	0.013	-2.48×10^5		
		4.18	0	0.009	0.454			106
				-0.002	0.474	3.80		
			4.02	0.082	0.368			107
				0.213	0.132	2274		
			15.85	1.279	-5.523			108
				-2.034	0.443	128		
			11.89	0.149	0.326			109
				0.258	0.131	1189		
		5.96	0	-84.26	85.26			111
				-37.24	0.526	9.15	25	
			4.02	0.064	0.457			112
				0.274	0.079	-1.30×10^4		
			7.87	0.098	0.384			113
				0.266	0.081	-3604		
			11.89	-4.06	0.387			114
				-4.50	0.248	685		
			15.84	0.141	0.380			115
				0.201	0.272	229		

Bead Diam (cm)	Mass	U_L	U_G	ε_G	ε_L	D	L_r	Run
0.32	2.25	7.99	0	0.045	0.568			116
				0.086	0.494	19.3	25	
			4.02	0.072	0.520			117
				0.183	0.320	277		
			7.87	0.099	0.507			118
				0.196	0.334	164		
			11.87	0.129	0.491			119
				0.214	0.337	900		
			15.82	0.172	0.454			120
				0.256	0.304	191		
		11.93	0	0.019	0.716			121
				0.010	0.732	29.2	41	
			4.28	0.087	0.668			122
				0.458	0.000	-		
			7.86	0.129	0.631			123
				0.269	0.380	1.56		
			11.86	0.175	0.583			124
				0.238	0.470	378		
	3	3.22	0	-0.126	0.487			126
				-0.042	0.337	28.4	25	
			4.00	0.119	0.342			127
				0.141	0.303	43.0		
			7.84	0.159	0.292			128
				0.174	0.264	150		
			11.82	0.197	0.279			129
				0.264	0.157	690		
			15.77	0.223	0.271			130
				0.246	0.229	297		
		4.18	3.99	0.089	0.367			132
				0.265	0.050	2.47×10^4		
			7.82	0.134	0.341			133
				0.321	0.004	-4.25×10^7		
			11.80	0.175	0.331			134
				0.348	0.019	-1.11×10^5		
			15.74	0.204	0.307			135
				0.258	0.208	652		
		5.96	0	0.012	0.529			136
				-0.005	0.560	3.83	33	
			3.98	0.075	0.435			137
				0.369	-0.093	-3587		
			11.77	0.149	0.392			139
				0.205	0.291	44.4		
		7.99	0	0.009	0.604			141
				0.030	0.567	9.66	39.5	
			3.99	0.069	0.508			142
				0.085	0.480	216		

Bead Diam (cm)	Mass	U_L	U_G	ϵ_G	ϵ_L	D	L_e	Run
0.32	3	7.99	7.82	0.121	0.490			143
				0,215	0.320	180	39.5	
			11.80	0.156	0.454			144
				0.315	0.168	-5512		
			15.72	0.189	0.468			145
				0.244	0.368	196		
		11.93	0	0.006	0.734			146
				0.019	0.710	29.1	62	
			3.99	0.110	0.622			147
				0.050	0.730	691		
			7.81	0.187	0.513			148
				0.155	0.570	139		
0.62	1.5	4.89	0	0.028	0.343			170
				0,051	0.301	63.6	8	
			4.03	0.092	0.349			171
				0.099	0.336	80.9		
			7.88	0.120	0.359			172
				0,164	0.280	54.1		
			11.89	0.162	0.359			173
				0.204	0.281	69.9		
			15.87	0.180	0.317			174
				0.199	0.282	111		
		5.96	0	-0.012	0.432			175
				0.047	0.324	53.7		
			4.03	0,101	0.404			176
				0.226	0.174	320		
			7.89	0.133	0.364			177
				0.231	0,183	-96.1		
			11.89	-120.06	121.057			178
				-54.529	0.286	197		
		7.99	0	0.209	0.354			179
				0.489	-0.162	1.75×10^4		

10.3 Nomenclature

C	concentration of tracer, gm/cm^3
d_p	particle diameter, cm
C(s)	Laplace transform of C(t)
C_s^n	n^{th} moment of transfer function, sec^n
D	dispersion coefficient, cm^2/sec

$F(s)$	system transfer function
$F'(s)$	first derivative of the transfer function
L_e	vertical distance between the two sets of electrodes, cm
M_S	mass of beads loaded to column, kg
Pe	Peclet number for the liquid phase, $\frac{u_L L_e}{D}$
s	Laplace transform parameter, sec^{-1}
t	time, sec
$\bar{t}$	mean (1st moment) of concentration curve
$\bar{t}_s$	1st moment of transfer function
U	superficial velocity
u	interstitial velocity
z	distance along column, cm
z_*	dimensionless distance along column, $\frac{z}{L_e}$
σ^2	variance (2nd moment) of concentration-time curve
ε_i	volume fraction (holdup)
σ_θ^2	dimensionless variance, σ^2/τ^2
τ	difference between mean residence times (also equal to L_e/u_L), sec

Subscripts

G	gas
L	liquid
S	solid
1	first measuring point
2	second measuring point

10.4 Literature References

1. Aris, R., "Notes on the Diffusion-Type Model for Longitudinal Mixing in Flow," Chem. Eng. Sci., 9, 266 (1959).

2. Bird, R.B., W.E. Stewart, and E.N. Lightfoot, "Transport Phenomena," pp. 183-188, Wiley, New York (1960).

3. Bischoff, K.B., "Notes on the Diffusion-Type Model for Longitudinal Mixing in Flow," Chem. Eng. Sci., 12, 69 (1960).

4. Bloxom, S.R., J.M. Costa, J. Herranz, S.R. Roth, and G.L. MacWilliam, "Determination and Correlation of Hydrodynamic Variables in a Three-Phase Fluidized Bed," ORNL/MIT-219 (November 1975).

5. Burck, G.M., K. Koichi, R.G. Markeloff, and S.R. Wilson, "Cocurrent Three-Phase Fluidized Bed, Part 2," ORNL/MIT-213 (May 19, 1975).

6. Christman, D.R., S.C. Loftus, and M.P. Rill, "Dispersion in a Three-Phase Fluidized Bed," ORNL/MIT-251 (March 1977).

7. Khosrowshahi, S., S.R. Bloxom, C. Guzman, and R.M. Schlapfer, "Cocurrent Three-Phase Fluidized Bed, Part 3," ORNL/MIT-216 (Sept. 29, 1975).

8. Levenspiel, O., "Chemical Reaction Engineering," 2nd ed., pp. 272-290, Wiley, New York (1972).

9. Levenspiel, O., and W.K. Smith, "Notes on the Diffusion-Type Model for the Longitudinal Mixing of Fluids," Chem. Eng. Sci., 6, 227 (1957).

10. Michelsen, M.L., and K. Ostergaard, Chem. Eng. Sci., 25, 583 (1970).

11. Ostergaard, K., and M.L. Michelsen, "On the Use of the Imperfect Tracer Pulse Method for Determination of Hold-up and Axial Mixing," Can. J. Chem. Eng., 47, 107 (1969).

12. Ostergaard, K., and M.L. Michelsen, "Hold-up and Axial Dispersion in Gas-Liquid Fluidized Beds, The Effect of Liquid Velocities and Particle Size," Am. Inst. Chem. Engrs., preprint 31D, Tampa (May 1968).

13. Ostergaard, K., and P.I. Theisen, "The Effect of Particle Size and Red Height on the Expansion of Mixed-Phase (Gas-Liquid) Fluidized Beds," Chem. Eng. Sci., 21, 413 (1966).

14. Saad, E.T., H.D. Ayala, W.M. Burke, and D.K. Clarkson, "Cocurrent Three-Phase Fluidized Bed, Part 1," ORNL/MIT-209 (March 21, 1975).

15. Van der Laan, E. Th., Chem. Eng. Sci., 7, 187 (1958).